NASA TECHNICAL NOTE

NASA TN D-2552

NASA TN D-2552

LARGE-SCALE WIND-TUNNEL TESTS ON AN ASPECT RATIO 2.17 DELTA-WING MODEL EQUIPPED WITH MIDCHORD BOUNDARY-LAYER-CONTROL FLAPS

by David G. Koenig and Victor R. Corsiglia

Ames Research Center

Moffett Field, Calif.

NATIONAL AERONAUTICS AND SPACE ADMINISTRATION • WASHINGTON, D. C. • DECEMBER 1964

LARGE-SCALE WIND-TUNNEL TESTS ON AN ASPECT RATIO 2.17 DELTA-WING MODEL EQUIPPED WITH MIDCHORD BOUNDARY-LAYER-CONTROL FLAPS

By David G. Koenig and Victor R. Corsiglia

Ames Research Center
Moffett Field, Calif.

NATIONAL AERONAUTICS AND SPACE ADMINISTRATION

For sale by the Office of Technical Services, Department of Commerce,
Washington, D.C. 20230 -- Price $3.00

LARGE-SCALE WIND-TUNNEL TESTS ON AN ASPECT RATIO 2.17 DELTA-WING MODEL EQUIPPED WITH MIDCHORD BOUNDARY-LAYER-CONTROL FLAPS

By David G. Koenig and Victor R. Corsiglia

Ames Research Center
Moffett Field, Calif.

SUMMARY

1906

The wing-fuselage model had midchord flaps which were 10 and 15 percent of the wing chord with hinge lines located along the 60- and 55-percent chord lines, respectively. Both flaps extended from 17 to 57 percent of the wing span. Deflecting the flaps left a cutout in the wing with the flap plan form outline. For midchord flap deflections more than 30°, blowing boundary-layer control was applied to the knee of the flap. The wing was also equipped with full-span constant-chord leading-edge flaps and partial-span 15-percent trailing-edge flaps which were deflected alone and in combination with the midchord flaps. Tests were made in and out of ground effect at zero sideslip over an angle-of-attack range of -2° to +22°. The Reynolds number for the tests was 13.7×10^6 and the Mach number was 0.10.

Lift increments due to 60° midchord flap deflections of 0.15 and 0.19 were measured at zero angle of attack with the 10- and 15-percent chord flaps, respectively. Pitching-moment changes were negligible for the midchord flap configurations investigated. Deflecting the leading-edge flap improved effectiveness of the flaps at the higher angles of attack. Calculations indicated that for a landing wing loading of 40 psf for an aircraft trimmed with either elevons or a canard, deflecting the 15-percent midchord flap 60° would reduce the landing speed 44 or 58 knots, respectively. Deflecting the trailing-edge flap in combination with the midchord flap for the canard controlled aircraft reduced landing attitude but not landing speed. For a take-off wing loading of 70 psf for an aircraft controlled either with elevons or a canard, calculations indicated that significant reductions in the take-off distance to an altitude of 35 feet and lift-off velocity could be obtained by deflecting the midchord flap to 30°.

INTRODUCTION

An important factor affecting landing and take-off performance of most aircraft is the lift available at a given take-off or landing attitude, the attitude being governed by aircraft geometry. Trailing-edge flaps are generally used to increase lift for a given attitude, but on aircraft with low-aspect-ratio wings with little or no trailing-edge sweep, maximum usable

flap deflection and, hence, trimmed lift increment for a given angle of attack are often limited by the size of the control used to trim the resulting pitch-down moments. Furthermore, the use of elevons on tailless aircraft would probably eliminate the possibility of using trailing-edge high lift devices.

One approach to the problem would be to use flaps located at some midchord position. The investigation at small scale reported on in reference 1 as well as an investigation using a small-scale semispan model indicated that midchord split flaps had little or no effect on pitching moment and produced very small lift increments relative to trailing-edge flaps of similar deflection, chord, and span. Further investigation using the semispan model indicated that a midchord flap installation which consisted of deflecting a center panel of the wing resulting in a cutout behind the deflected panel produced considerably more lift than did a split flap of similar plan form and location. In addition, a flap-hinge position was found near the 55-percent chord line for which the flap had no effect on pitching moment but produced a significant lift increment.

A subsequent investigation was made with a large-scale delta-wing and fuselage model which had a wing plan form similar to that of the semispan model. The wing had an aspect ratio of 2.17 and was equipped with 10- and 15-percent-chord midchord flaps with hinges located at the 60- and 55-percent chord lines, respectively. The wing was also equipped with constant chord leading-edge flaps and 15-percent-chord trailing-edge flaps which were tested in combination with the midchord flap. The effectiveness of the flap at large deflections was investigated with boundary-layer control applied to the flap knee as required to minimize flow separation over the flap.

NOTATION

b	span, ft
c	chord, ft
$\bar{c}$	mean aerodynamic chord, $\frac{2}{S}\int_0^{b/2} c^2\,dy$, ft
C_D	drag coefficient, $\frac{D}{qS}$
C_{D_o}	model minimum drag coefficient
C_L	lift coefficient, $\frac{L}{qS}$
C_m	pitching-moment coefficient, $\frac{M}{qS\bar{c}}$
C_μ	blowing-momentum coefficient, $\frac{W/g}{qS} V_j$
g	acceleration of gravity, 32.2 ft/sec^2

h	height of moment center above the ground, ft
l_c	distance from $\frac{\bar{c}_w}{4}$ to canard hinge line, ft
L	lift, lb
M	pitching moment about the $\frac{\bar{c}}{4}$ station, ft-lb
p	free-stream static pressure, lb/sq ft
P	wing-surface pressure coefficient, $\frac{p_1 - p}{q}$
q	free-stream dynamic pressure, lb/sq ft
S	total wing area unless otherwise indicated by subscript, sq ft
S_c	total canard area, sq ft
S_{35}	take-off distance to an altitude of 35 ft, ft
T	thrust, lb
V	airspeed, knots
V_j	jet velocity, assuming isentropic expansion, ft/sec
W	airplane gross weight, lb, or weight rate of flow, lb/sec
x	chordwise location measured parallel to plane of symmetry, ft
y	distance measured perpendicular to the model plane of symmetry, ft
α	angle of attack of the wing, deg
δ_f	trailing-edge flap deflection, normal to hinge line, deg
δ_{mf} and δ'_{mf}	midchord flap deflection normal to the hinge line, see figure 2(b), deg
δ_n	leading-edge flap deflection, normal to the hinge line, deg
Δ	incremental value, with α constant unless noted otherwise
η	dimensionless spanwise location, $\frac{2y}{b}$
Λ	sweep angle, deg

Subscripts and Abbreviations

BLC	boundary-layer control
f	flap
l	local surface (pressure)
LO	condition corresponding to lift-off during take-off
LE	leading edge
MF	1, 2, 3, 4, and 5 midchord flap configuration, see figure 2(b)
R	condition corresponding to rotation during take-off
TE	trailing edge
u	uncorrected

MODEL AND APPARATUS

The model is shown installed on the conventional support system in the 40- by 80-foot wind tunnel in figures 1(a) and (b) and on the ground plane system in figure 1(c). To study ground effect, the model was lowered toward the wind-tunnel floor.

A two-view sketch of the model is presented in figure 2(a) and pertinent details are listed in table I. The model consisted of a wing, fuselage, and vertical tail. The wing was equipped with leading-edge, midchord, and trailing-edge flaps. The flap plan forms are defined in figure 2(a). The leading- and trailing-edge flaps were plain. The hinge of the leading-edge flap was located near the wing lower surface and that of the trailing-edge flap, on the wing chord plane.

A sectional view of the midchord flap is presented in figure 2(b). The deflected midchord flap formed a cutout in the wing behind the deflected flap. The hinge lines of the 10- and 15-percent chord flaps were at 60- and 55-percent chord, respectively, with the aft edge of the cutout or lip fixed at 70-percent chord. A nozzle for boundary-layer control was installed in the flap radius as shown in figure 2(c). Boundary-layer-control air was supplied by a centrifugal type compressor and was ducted to the nozzle via a duct located inside the flap. Mass rate of air flow was measured by means of a standard ASME flat-plate orifice permanently installed in the ducting system.

For a portion of the investigation, a flap that would be formed by the rotation of a full depth portion of the wing was simulated, as shown in

figure 2(b), by adding a separate panel of wedge cross section to the flap lower surface and by replacing the rounded-wing lip with a lip of rectangular cross section.

Pressure orifices were installed on the wing along a streamwise wing station at 50-percent wing semispan. The orifices on the flaps were located at this station with the flaps retracted.

TESTS AND PROCEDURE

Force and moment data were obtained for the model through an angle-of-attack range from -2° to $+22^{\circ}$. Tests were made at zero sideslip with the model in and out of the presence of the ground. Table II is an index to the configurations tested.

For a few model configurations, force and moment data were obtained with varying C_{μ} at constant nominal angle of attack. For the variable angle-of-attack tests with BLC on, the weight rate of flow was held approximately constant at a value slightly above the critical value determined by the results of the variable C_{μ} tests at $\alpha = 0^{\circ}$ for a corresponding midchord flap deflection.

All tests were made at a free-stream dynamic pressure of 15 pounds per square foot, which corresponds to a Mach number of 0.10 and a Reynolds number of 13.7×10^{6} based on the wing mean aerodynamic chord.

DATA REDUCTION AND CORRECTIONS

Forces and moments for the model were derived from the mechanical scale data for both systems of model support. The moment data were referred to the $0.25\bar{c}$ point and are presented as such unless otherwise noted.

For data obtained on the conventional support system, no corrections for strut tip tares have been applied except for the data used in the derivation of trim characteristics. The following wind-tunnel wall corrections were made to the data:

$$\Delta\alpha = 1.06\ C_{L_u}$$

$$\Delta C_D = 0.0184\ C_{L_u}{}^2$$

The data obtained on the ground-plane system were not corrected for the wind-tunnel wall but those obtained at the highest ground height were corrected to correspond to out of ground effect. The wind-tunnel wall corrections used in this case were identical to those for the conventional support system.

All data obtained on the ground-plane system were corrected for strut tare and wind-stream angularity as follows:

$$\alpha = \alpha_u + \alpha_\alpha$$

$$C_L = C_{L_u} - C_{D_u} \sin \alpha_\alpha$$

$$C_D = C_{D_u} + C_{L_u} \sin \alpha_\alpha + \Delta C_{D_{tare}}$$

$$C_m = C_{m_u} + \Delta C_{m_{tare}}$$

where α_α was 1.7° and 2.0° for $h/c = 0.32$ and 0.66, respectively. The strut tares, $\Delta C_{D_{tare}}$ and $\Delta C_{m_{tare}}$, were based on system calibrations with struts alone. The stream-angularity corrections, 1.7° and 2.0°, were determined as the deviations in model angle of attack from geometrical zero angle of attack required to obtain $C_L = 0.03$ (the value obtained on the conventional support system).

RESULTS AND DISCUSSION

Basic Force and Moment Data

Table II may be used as an index to figures 3 through 9. Lift, drag, and pitching-moment data for the model with the midchord flap deflected are presented in figures 3 through 7. Data for the model with the midchord flap undeflected are presented in figure 8. Results of tests of the model on the ground-plane support system with and without the midchord flap deflected are presented in figure 9. Variations of C_L with C_μ measured for several test conditions are presented in figure 10. The tick marks placed on the curves indicate the approximate C_μ for complete flow attachment as determined by surface pressure distribution.

Effect of the Midchord Flap on the Aerodynamics of the Model

Chordwise loading.- Chordwise pressure distributions at the 50-percent semispan station are presented in figure 11 for the 15-percent chord flap. The values of x/c used for the flap pressure measurements correspond to the orifice locations measured with all wing flaps retracted.

The effect of the midchord flap can be seen in figure 11. The wing section with the midchord flap deflected can be considered as two tandem airfoils. The circulation on the forward airfoil resulting from the deflection of the midchord flap induces a downward loading on the portion of the wing behind the midchord flap. Evidence of this is shown in figure 11 where more negative pressure differentials in a downward direction on the rear portion of the wing were generally obtained with BLC on than with BLC off.

The exception was the leading edge of the rear portion of the wing where flow separation evidently occurred on the lower surface with BLC on, reducing the pressure differential. The increased lift on the forward portion of the wing is sufficient to offset the negative lift induced on the aft portion, causing a net gain in lift. Correspondingly, the center of pressure is located farther forward on the airfoil with a midchord flap than on an airfoil with a trailing-edge flap.

Increasing angle of attack reduces the pressure differential between the upper and lower surface on the wing aft of the midchord flap. This probably reduces the quantity of air flowing through the wing cutout and reduces the flap lift increment with increases in angle of attack.

The effect of flap chord and position on lift and moment.- The ratios of lift and moment changes to flap deflection for several combinations of flap chord and chordwise position with the model at $\alpha = 0^{\circ}$ are plotted in figure 12 versus chordwise location of the flap hinge lines. To augment the data of the present tests, small-scale data and some calculated results are also presented. The small-scale data were obtained using a semispan model with wing plan form and flap installations similar to those of the large model. Measured values for the trailing-edge flaps were corrected to a spanwise extent corresponding to the midchord flap by adjusting the values in proportion to the corresponding wing areas spanned by the flaps.

The effect of flap chord and chordwise position on the lift and moment changes due to flap deflection is indicated in figure 12 by the curves faired through the large-scale values following the trends indicated by the small-scale data (for a 15-percent chord flap). The flap hinge locations for zero pitching-moment change with flap deflection appear to be about 62- and 57-percent wing chord for the 10- and 15-percent chord flaps, respectively. It also appears that for these flap locations (for $\Delta C_m/\delta_{mf} = 0$), flap lift increments obtained with either the 10- or 15-chord midchord flaps were approximately one-third those which would be obtained with trailing-edge flaps of equivalent plan form and deflection.

Lift increment.- The variation of midchord flap lift increment with flap deflection for $\alpha = 0$ is shown in figure 13 for both the 10- and 15-percent chord flaps. Fairing of the data representing BLC off was made with the assumption that BLC was not required for flap angles below 30°. It is evident for both flap chords that with the flaps deflected 60° the flap lift increment obtained with BLC on was approximately twice that obtained with BLC off. With BLC on, the lift increments obtained were approximately 0.15 and 0.19 for the 10- and 15-percent chord flaps, respectively.

The variation of flap lift increment with angle of attack is presented in figure 14 for the 15-percent chord flap deflected in combination with several leading-edge flap deflections. The decreasing flap lift increments with angle of attack (see figs. 6 and 8) reflect the reduced lift curve slopes typical of all midchord flap configurations of the present large-scale tests. By comparison, figure 8 indicates the lift increment of a trailing-edge flap is relatively constant with angle-of-attack change until either the

wing or flap is stalled. The major effect of the leading-edge flap on the midchord flap lift increment was to increase the angles of attack at which a rapid loss in lift increment occurs.

Figure 15 shows the effect of blunting both the midchord flap trailing edge and the lip of the rear portion of the wing. As shown by figure 15, for both $\delta_{mf} = 45^\circ$ and 60°, either adding the wedge to the flap lower surface or blunting the wing lip slightly reduced the flap lift increment and at the same time reduced the flap lift increment about 16 percent for angles of attack near 12°. As shown by the sketch of figure 2(b), the effect of blunting both flap and wing lip is to simulate a flap formed by rotating a full depth wing panel by an angle, δ'_{mf}.

The effect of trailing-edge flap deflection on the midchord flap lift increment is shown in figure 16 for $\delta_{mf} = 60^\circ$ with and without BLC. With BLC on, deflecting the trailing-edge flaps to 20° resulted in a reduction of midchord flap lift increment equivalent to percentage losses of 23 and 35 percent for $\alpha = 0^\circ$ and 12°, respectively.

Aircraft Performance With a Midchord Flap

Basic trim data.- Characteristics of the model in trimmed level flight are presented in figures 17 and 18 for an elevon- and canard-controlled aircraft, respectively. For the elevon-controlled characteristics, the trailing-edge flap was used for pitch control and the test data were extrapolated as required to negative values of flap deflection, δ_f, for use in the derivation. For the canard-controlled characteristics, a canard volume, $S_c l_c / S\bar{c}$, of approximately 0.16 was assumed with corresponding trim lift and drag increments equivalent to an aspect-ratio-2 delta wing with a total area of about 11 percent of that of the wing. Canard-fuselage gap effects, mutual interference between the canard and the fuselage, and the canard influence on the wing were not considered. The static margin near $\alpha = 0^\circ$ for the resulting trim data varied from 1 to 4 percent depending on wing configuration.

Characteristics during landing approach.- The variation of thrust-to-weight ratio with airspeed is presented in figures 19 and 20 for an elevon- and canard-controlled aircraft, respectively, with a wing loading of 40 psf. The trim data of figures 17 and 18 were used to derive these results assuming no thrust contribution to lift and using a landing-gear drag increment of 0.012. Minimum speed for landing approach are indicated on the curves and are based on the criteria of $\partial(T/W)/\partial V \geqq 0$.

The data of figures 19 and 20 indicate that with the leading-edge flaps undeflected, the deflection of the 15-percent chord midchord flap to 60° reduced the landing-approach speeds by 44 and 58 knots for the elevon- and canard-controlled aircraft, respectively. The corresponding angle of attack decreased from approximately 6° to 5° for the elevon-controlled aircraft and increased from 6° to 7° for the canard-controlled aircraft. Further reductions in landing speed were obtained with the leading-edge flap deflected for the midchord and trailing-edge flap deflections investigated. The deflection

of the trailing-edge flap alone or in combination with the midchord flap with the canard used as control had little effect on landing-approach speeds but reduced the approach angle of attack by about 3°. A desirable landing configuration for the canard-controlled aircraft would therefore be a combination of both midchord-flap and trailing-edge flap deflections which, as shown in figure 20(c), would result in a landing attitude of 8° corresponding to a landing-approach speed for neutral speed stability $[\partial(T/W)/\partial V = 0]$ of 133 knots.

Take-off performance.- The effect of midchord-flap deflection on take-off performance was investigated for a gross weight of 450,000 lb and wing loading of 70 psf for both the elevon- and canard-controlled aircraft. Computed take-off distances are presented in figure 21 as functions of thrust-to-weight ratio T/W. The computed distances represent "hot day" values and all values of T/W presented represent equivalent standard-day sea level static thrust. Pertinent details and assumptions used in the computation are presented in appendix A. In order to expedite calculation, two simplifying assumptions for calculating transition were made, namely, constant ground effect for altitudes to 35 feet, and constant angle of attack during transition.

The results of the calculations presented in figure 21 demonstrate that using the midchord flaps can improve take-off performance of either the canard- or elevon-controlled aircraft. As shown in figure 21(a), for the elevon-controlled aircraft, deflecting the midchord flaps to 30° for a maximum rotation angle, $\alpha_{LO} = 10^{\circ}$, total take-off distance to an altitude of 35 feet was reduced by approximately 800 feet for the values of T/W considered with an accompanying reduction in lift-off velocity of about 15 knots. These improvements were slightly less for $\alpha_{LO} = 12^{\circ}$. For the canard-controlled aircraft, data shown in figure 21(b) indicate that improvements in take-off performance obtained with the midchord flap deflected 30° approach those which would be obtained with the trailing-edge flap deflected 10°. For the maximum rotation angle, $\alpha_{LO} = 10^{\circ}$, average reductions in take-off distance of 600 and 900 feet were obtained with the midchord flaps and the trailing-edge flaps, respectively. At the higher rotation angle ($\alpha_{LO} = 12^{\circ}$), the principal improvements were in the reduction in lift-off velocity of 10 or 17 knots for the midchord or trailing-edge flaps, respectively.

CONCLUDING REMARKS

Results of large-scale wind-tunnel tests on a low-aspect-ratio delta-wing fuselage model equipped with midchord flaps indicate that significant lift increments could be obtained with negligible pitching-moment changes for a moment center located at the quarter-chord point of the mean aerodynamic chord. Flap lift increment was approximately doubled by the use of BLC for 60° flap deflection resulting in values of lift increment of 0.15 and 0.19 for the 10- and 15-percent chord flaps, respectively. Deflecting the leading-edge flaps improved effectiveness of the flaps at the higher angles of attack.

Results for the model trimmed by means of either elevon or a canard for a landing wing loading of 40 psf indicated that landing speeds corresponding to the speed stability criterion, $\partial(T/W)/\partial V = 0$, could be reduced by 44 and 58 knots with the aircraft trimmed by elevons or a canard, respectively. Reductions in landing-approach attitude but little change in landing speed can be made for the canard-controlled aircraft with the use of trailing-edge flaps in combination with the deflected midchord flap. Take-off calculations for an elevon-controlled aircraft with a wing loading of 70 psf indicated that the midchord flap deflected to 30° without BLC would reduce take-off distances by about 800 feet and lift-off velocities by about 15 knots. For canard-controlled aircraft of the same wing loading, the magnitude of these reductions approach those obtained with a trailing-edge flap deflected 10°.

Ames Research Center
National Aeronautics and Space Administration
Moffett Field, Calif., Sept. 18, 1964

APPENDIX A

TAKE-OFF COMPUTATION

Four engine take-off distances were computed using the subject test data for the model in and out of ground effect. The basic differential equations of motion were integrated on an electronic computer with the take-off sequence as follows:

1. Standing start to velocity for rotation, V_R.

2. Airspeed, V_R, to lift-off velocity, V_{LO}, with the aircraft rotating to a maximum angle of attack, α_{LO}, attained simultaneously with the reaching of V_{LO}.

3. Transition from a point for V_{LO} (C_L, C_D, constant) to an altitude of 35 feet (V_{LO} was defined as that velocity for which $W = L_{LO} + T \sin \alpha_{LO}$).

The problem constants used in calculating take-off distance are as follows:

Gross weight, W	450,000 lb
Atmosphere	sea level, 85° F
Wing loading (constant)	70 psf
Rolling friction coefficient	0.02
Rotation rate	3°/sec
Thrust incidence	0°
Ground roll, α	0°

The values of gross weight and wing loading are typical of proposed supersonic transport designs.

The aerodynamic data used for conditions of $V \geqq V_R$ were derived from the trim data of figures 17 and 18 by adjusting the trim lift and drag for ground effect using increments of C_L and C_D obtained from the data of figure 9. These increments were added directly for corresponding angles of attack. For ground roll prior to reaching V_R, data for the model at $\alpha = 0°$ with the controls neutral were used in the calculations.

Values of thrust used for the calculation are presented in figure 22. The values are believed to reflect typical changes caused by ambient air temperature and airspeed for an engine with a 1.5 bypass ratio and augmentation.

Both the JC 805 fan jet engine and a turbojet engine, such as the J57, were investigated. A design procedure similar to those outlined in reference 4 was used to calculate thrust losses due to engine compressor airbleed to supply the midchord flap BLC system. The nozzle area was sized for the lower available compressor-bleed pressure during landing, using a value of

C_μ = 0.022, a duct loss of 30 percent, and a 3° descent slope at an airspeed of 140 knots. For take-off, the thrust losses due to airbleed were computed for an airspeed of 160 knots, a standard-day value of T/W = 0.42, and assuming no throttling to reduce excess duct pressure. The thrust losses from compressor bleed were 2.3 and 1.1 percent for the turbojet and fan jet, respectively. The lower thrust loss was used in adjusting the thrust data of figure 22 for application to the take-off calculations for the 45° mid-chord flap deflection. No bleed air is necessary with flap deflected 30°.

REFERENCES

1. Spencer, Bernard J.: Low-Speed Aerodynamic Characteristics of a Canard Airplane Configuration Having Split Flaps Located Ahead of the Wing Trailing Edge and Leading- and Trailing-Edge Flaps on the Canard Control. NASA TN D-1245, 1962.

2. DeYoung, John: Theoretical Symmetric Span Loading Due to Flap Deflection for Wings of Arbitrary Plan Form at Subsonic Speeds. NACA TR 1071, 1952.

3. James, Harry A., and Hunton, Lynn W.: Estimation of Incremental Pitching Moments Due to Trailing-Edge Flaps on Swept and Triangular Wings. NACA RM A55D07, 1955.

4. Kelly, Mark W., and Tolhurst, William H., Jr.: Full-Scale Wind-Tunnel Tests of a 35° Sweptback Wing Airplane With High-Velocity Blowing Over the Trailing-Edge Flaps. NACA RM A55I09, 1955.

TABLE I.- GEOMETRIC DATA

Wing	
Area S, ft^2	445.63
Span, b, ft	31.10
$\bar{c}$, ft	19.11
Aspect ratio	2.17
Taper ratio	0
Airfoil section	NACA 0003-03
Root chord, ft	28.67
Sweep c/4, deg	50.4
LE, deg	59.0
TE, deg	-10.0
Sweep of flap hinge, deg	
LE flap	59.0
TE flap	5.7
MF 1(c_f/c = 0.15)	33.2
MF 4(c_f/c = 0.10)	29.3
Flap area, sq ft	
LE	46.6
TE	46.80
MF 1(c_f/c = 0.15)	33.8
MF 4(c_f/c = 0.10)	22.50

FUSELAGE COORDINATES

Station, ft	Radius, ft	Station, ft	Radius, ft
0	0.02	36	2.02
2	.30	38	2.03
4	.53	40	2.03
6	.72	42	2.03
8	.88	44	2.03
10	1.03	46	2.01
12	1.18	48	1.98
14	1.33	50	1.93
16	1.46	52	1.87
18	1.58	54	1.77
20	1.68	56	1.63
22	1.76	58	1.48
24	1.83	60	1.27
26	1.88	62	1.03
28	1.92	64	.77
30	1.95	66	.43
32	1.98	67.29	.02
34	2.00		

TABLE II.- INDEX TO BASIC DATA AND MODEL CONFIGURATIONS

Figure no.	Notation or $h/\bar{c}$	δ_n, deg	δ_f, deg	δ_{mf}, deg	BLC
Conventional support system					
3(a)	MF 1(c_f/c = 0.15)	0	0	30, 45	Off
(b)				45, 60	Off, on
4		30		45, 60	Off, on
5(a)		45		45, 60	Off, on
(b)				71	Off, on
(c)			10, 20	45	Off, on
(d)			10, 20	60	Off, on
6(a)	MF 1, 2, 3 (c_f/c = 0.15)		0	45	Off
(b)					On
(c)				60	Off
(d)					On
7(a) and (b)				0	Off
	MF 4(c_f/c = 0.10)			45, 60	Off, on
	MF 5(c_f/c = 0.10)			60	Off, on
8(a)	Base runs	0, 30, 45	0	0	Off
		45	10, 20		
(b)		0, 45	10		
Ground plane system MF 4(c_f/c = 0.10)					
9(a)	0.32, 0.66, ∞	45	0	0	Off
(b)	0.32, 0.66, ∞			60	On
(c)	0.32		0, 10, 20	0	Off
(d)				60	On

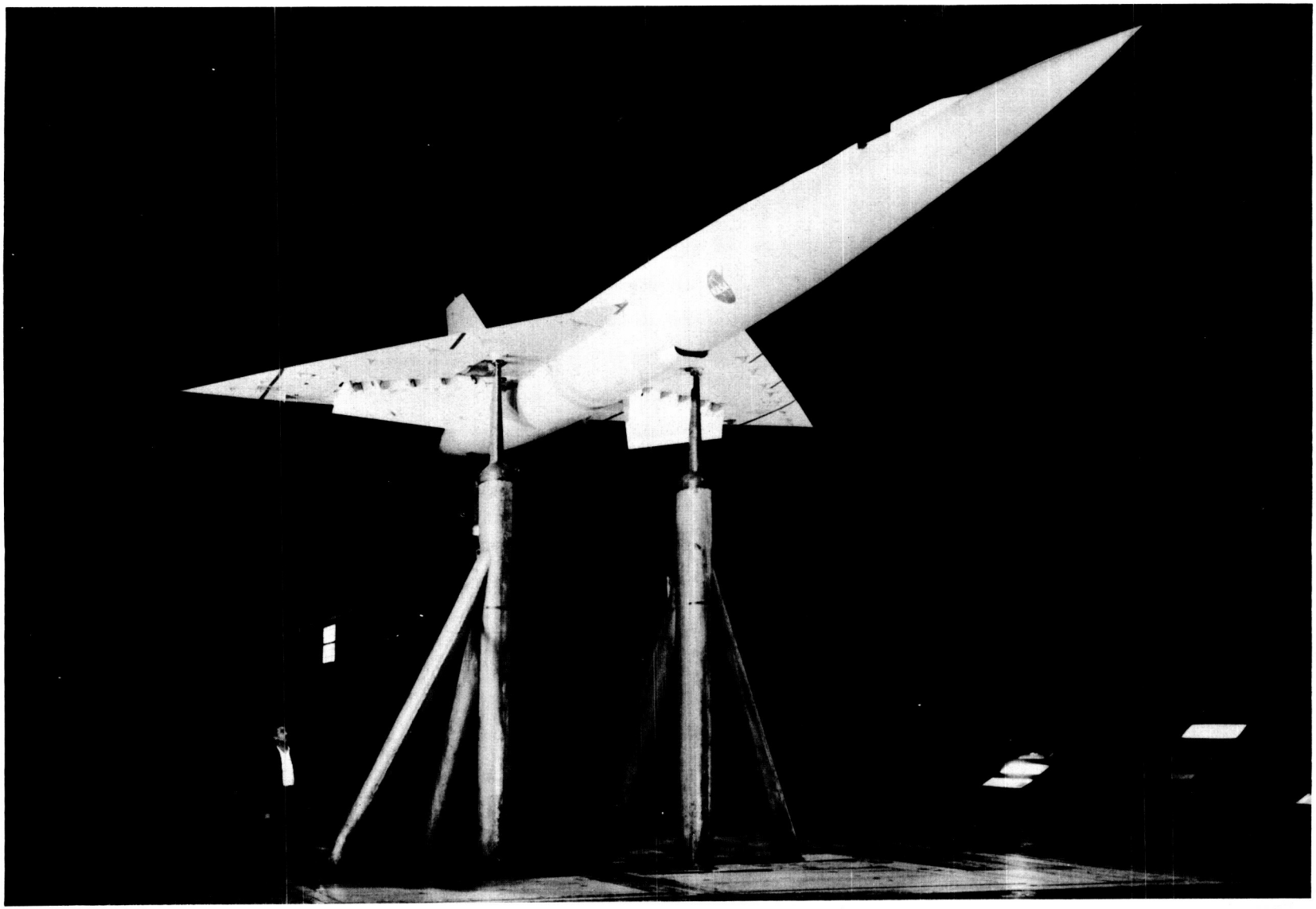

A-30624

(a) Conventional support system, front view.

Figure 1.- The model shown mounted in the Ames 40- by 80-Foot Wind Tunnel.

A-30625

(b) Conventional support system, rear view.

Figure 1.- Continued.

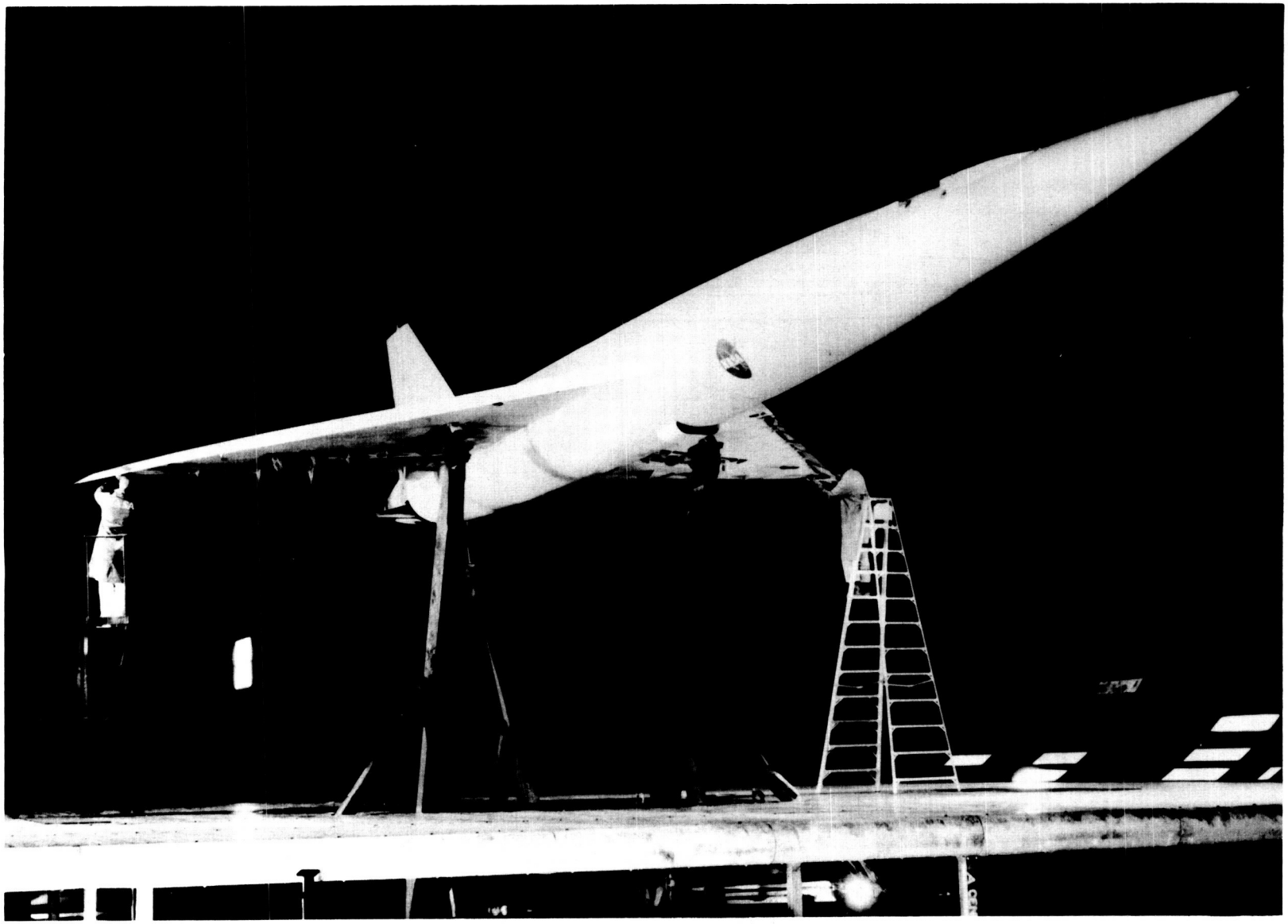

A-31801.1

(c) Ground-plane system, front view.

Figure 1.- Concluded.

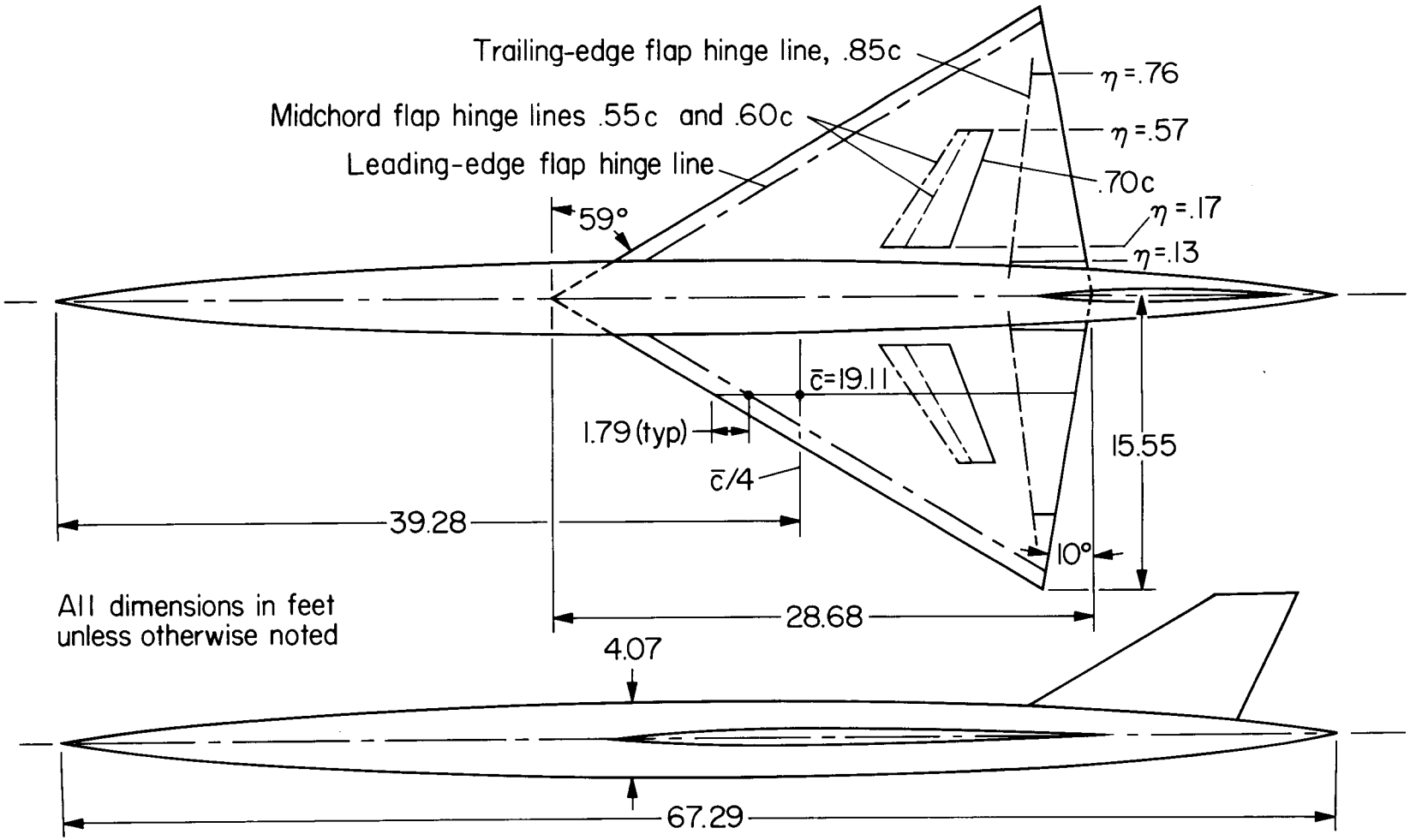

(a) Two view of the model.

Figure 2.- Geometric details of the model.

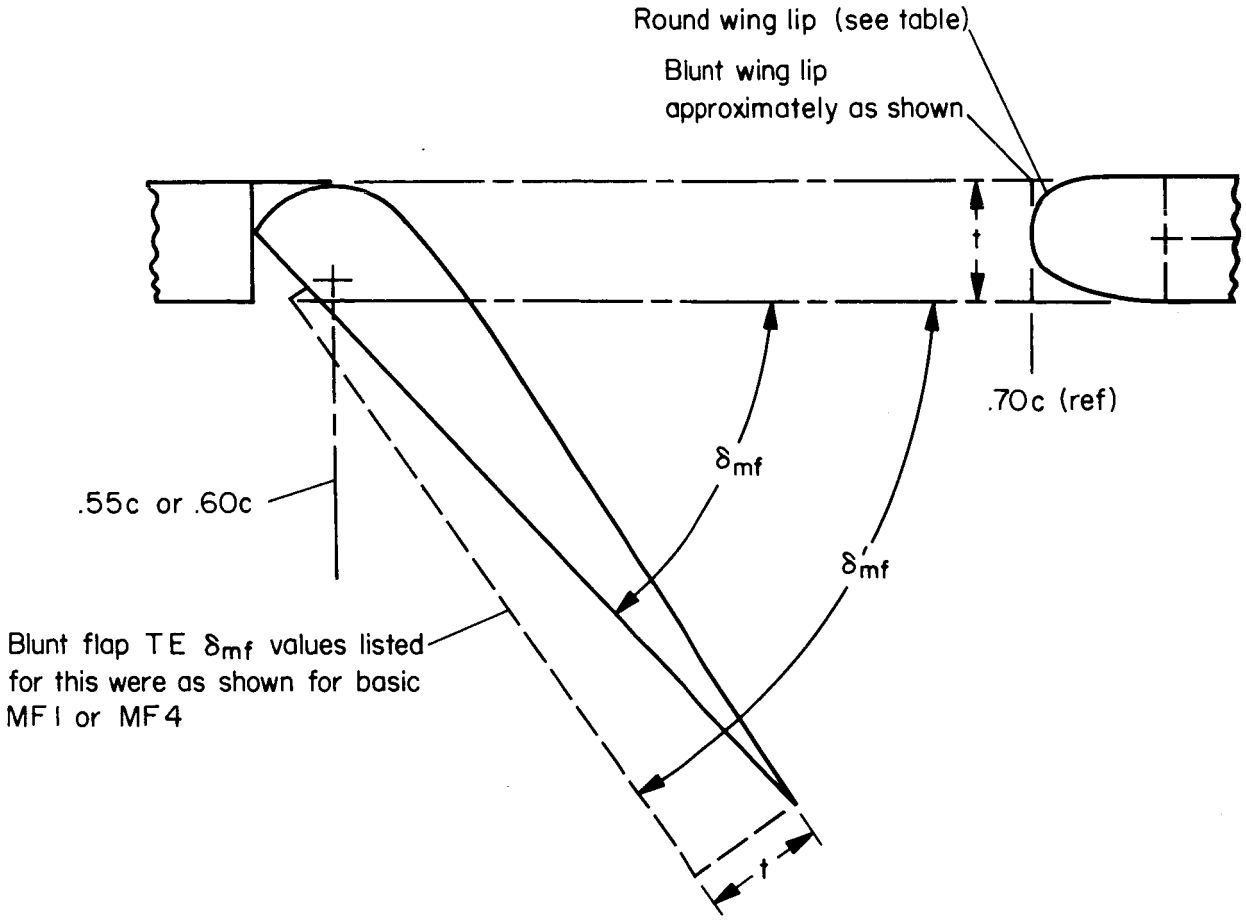

Notation	% c		Flap TE	Lip		Round lip (streamwise) ordinates, inches		
	Hinge location	Flap chord				Station	Lower	Upper
MF1	55	15	Taper	Round	η = .17	0	.80	.80
						.5	-.50	1.98
						1.0	-1.02	2.30
MF2			Blunt	Round		3.0	-2.01	2.68
						5.0	-2.44	2.58
MF3			Blunt	Blunt		7.0	-2.56	2.48
					η = .57	0	.41	.41
MF4	60	10	Taper	Round		.25	-.25	1.01
						.51	-.84	1.17
						1.53	-1.03	1.36
MF5			Taper	Blunt		2.55	-1.24	1.31
						3.56	-1.30	1.30

(b) Section of midchord flap perpendicular to the hinge line.

Figure 2.- Continued.

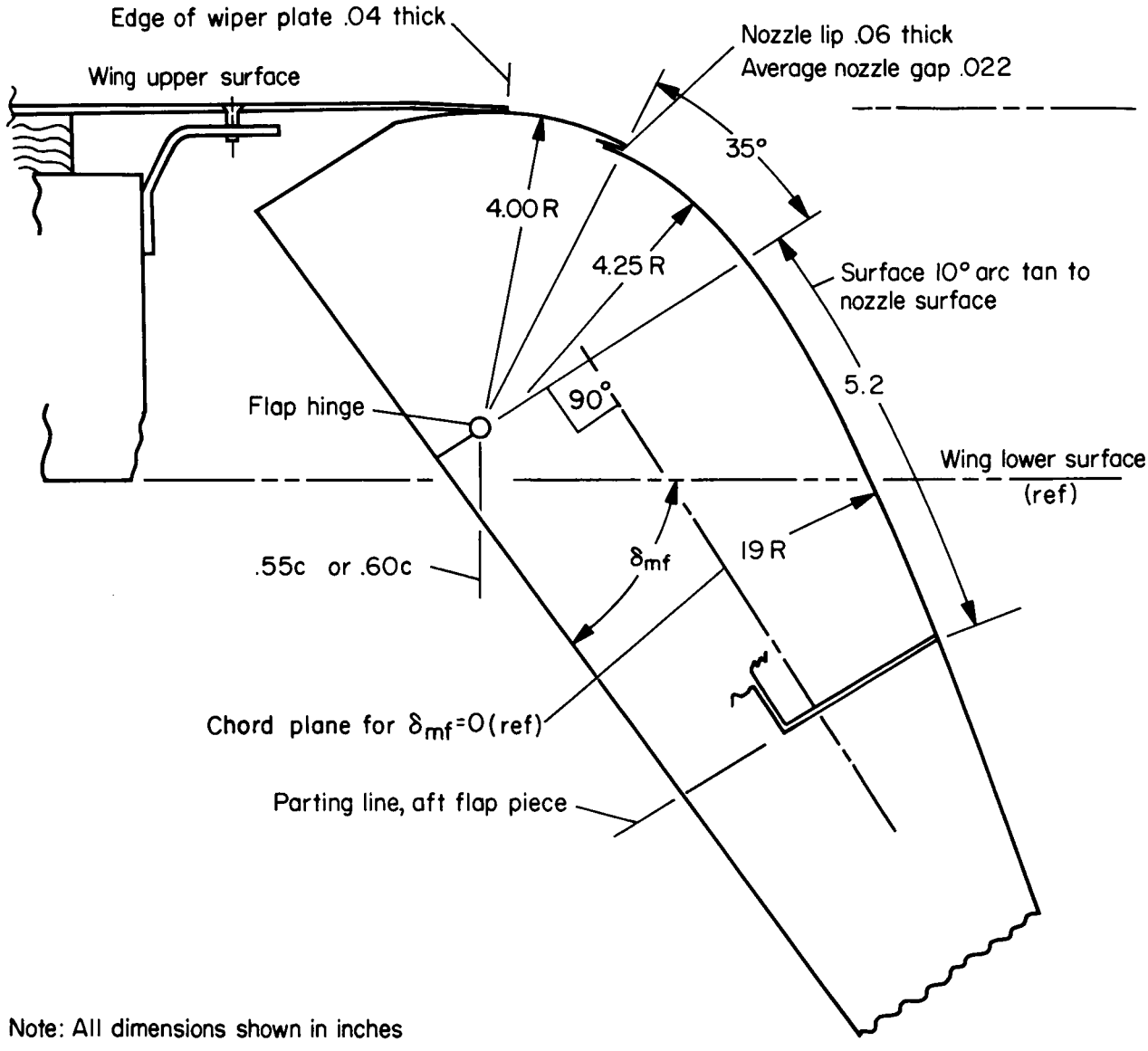

(c) Details of the nozzle profile; typical of all midchord flap installations; section perpendicular to hinge line.

Figure 2.- Concluded.

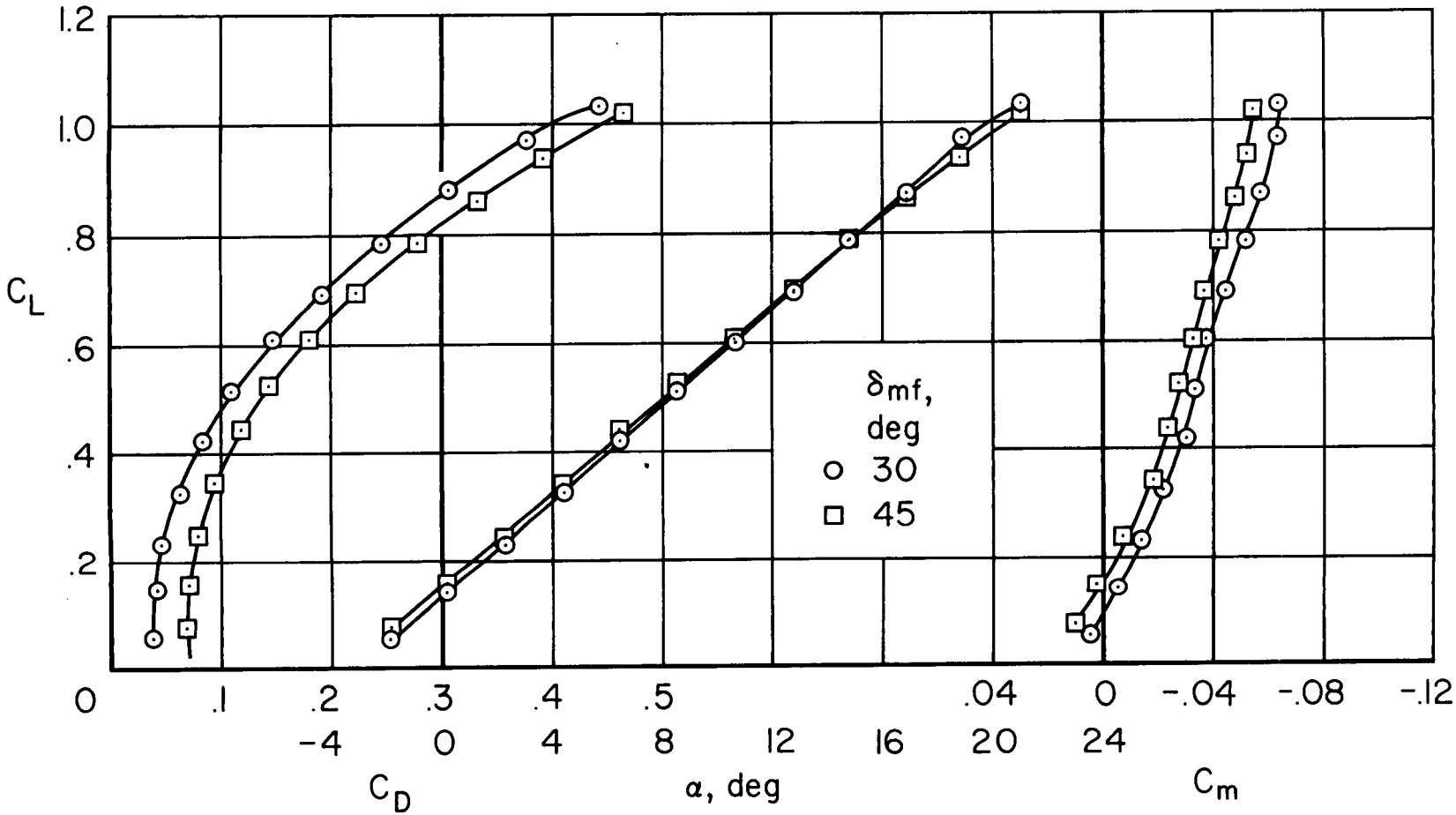

(a) BLC off.

Figure 3.- Characteristics of the model with the leading-edge flaps undeflected; $\delta_n = 0^\circ$, MF 1($c_f/c = 0.15$), $\delta_f = 0^\circ$.

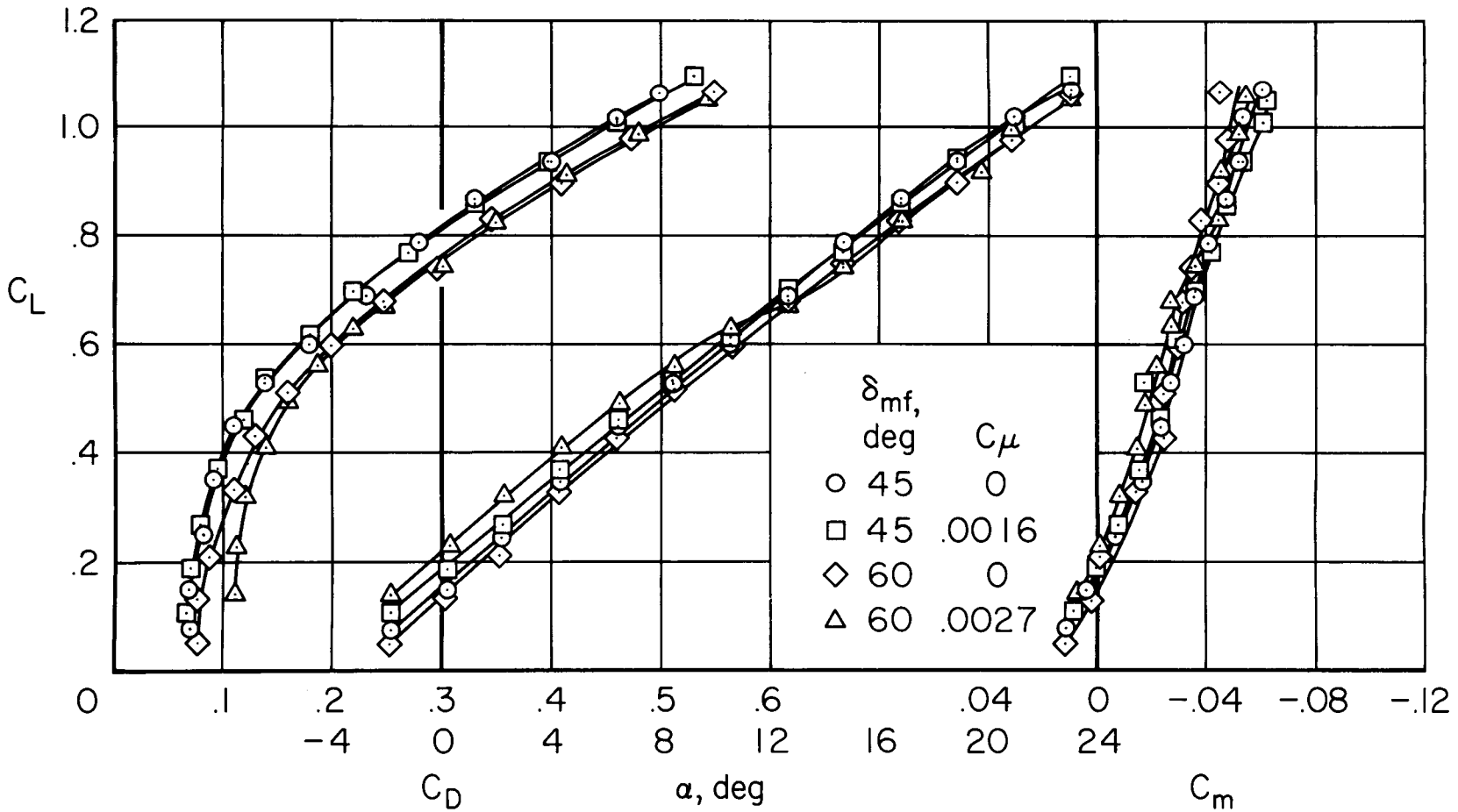

(b) BLC off and on.

Figure 3.- Concluded.

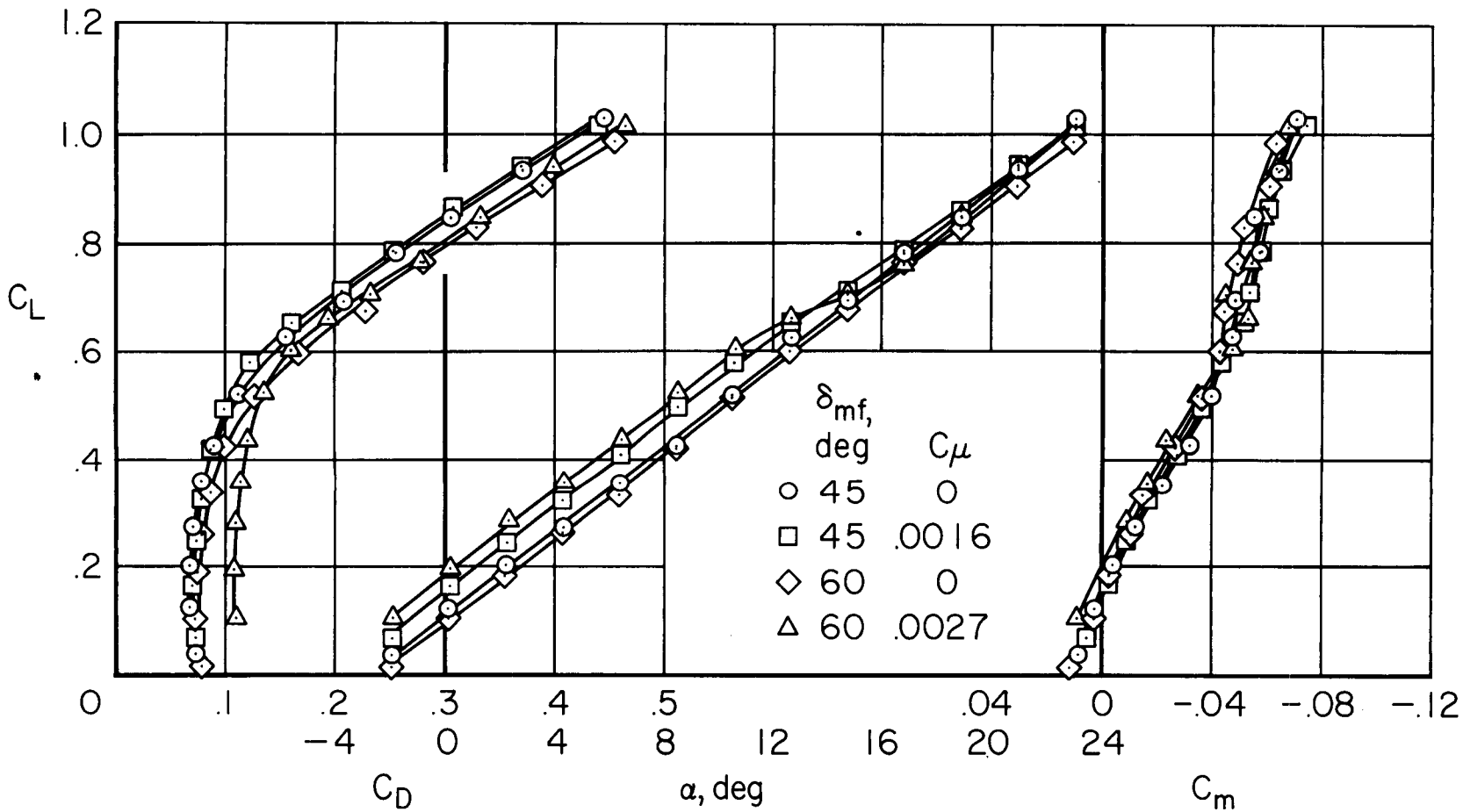

Figure 4.- The characteristics of the model with leading-edge flaps deflected 30°; MF 1(c_f/c = 0.15), δ_f = 0°.

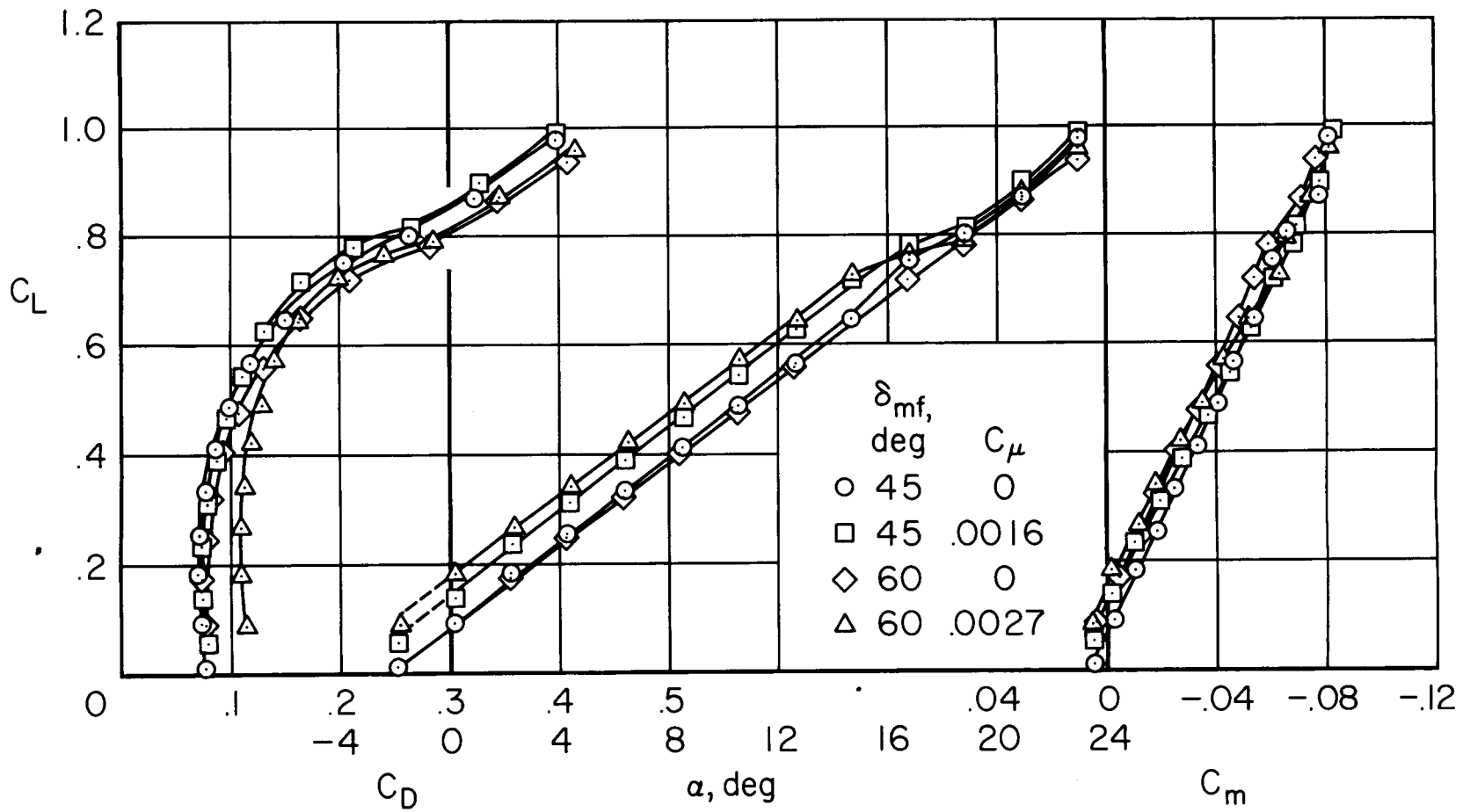

(a) $\delta_f = 0°$; $\delta_{mf} = 45°$ and $60°$.

Figure 5.- Characteristics of the model with the leading-edge flap deflected 45°; MF 1($c_f/c = 0.15$).

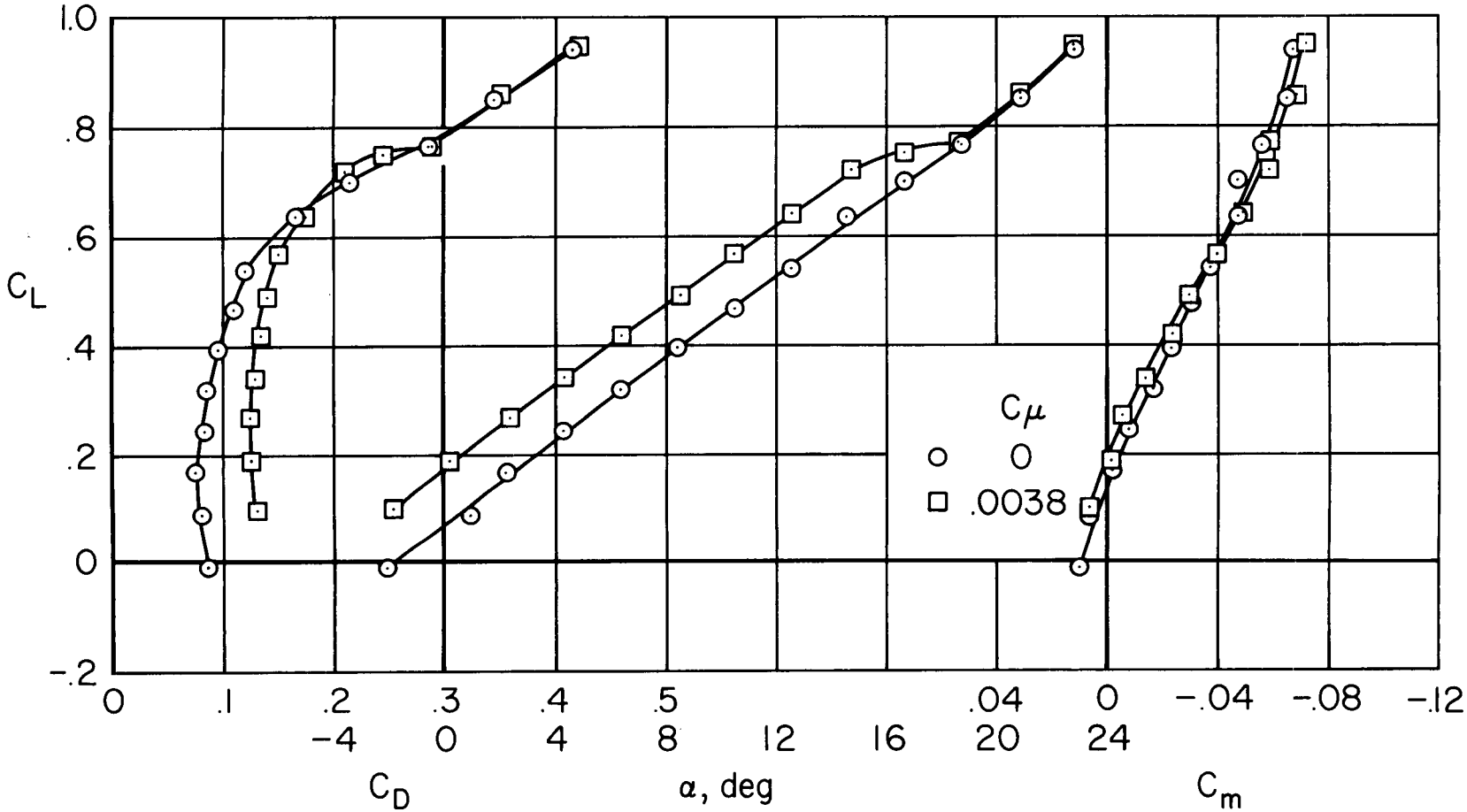

(b) $\delta_f = 0^\circ$; $\delta_{mf} = 71^\circ$.

Figure 5.- Continued.

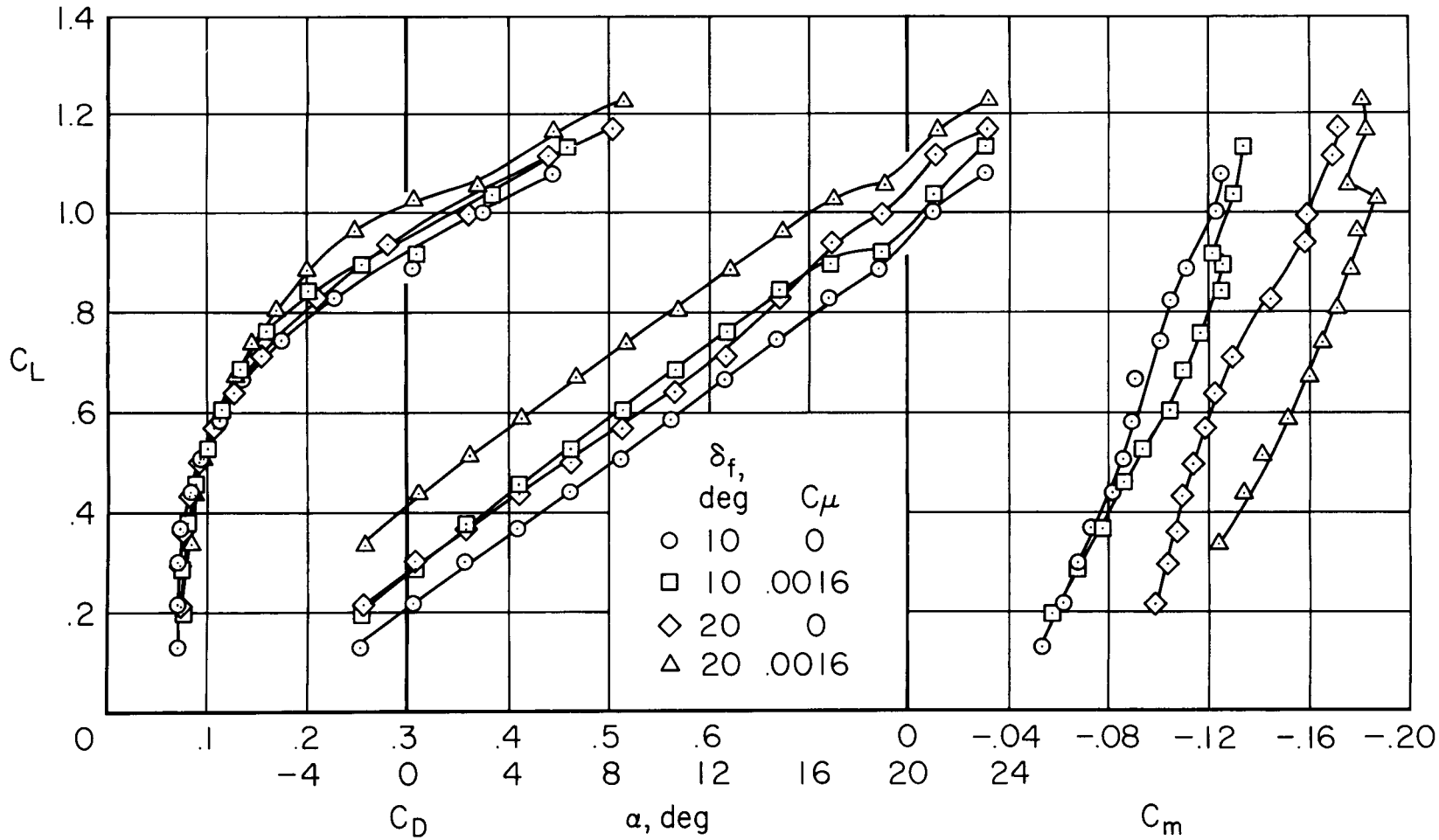

(c) $\delta_{mf} = 45°$.

Figure 5.- Continued.

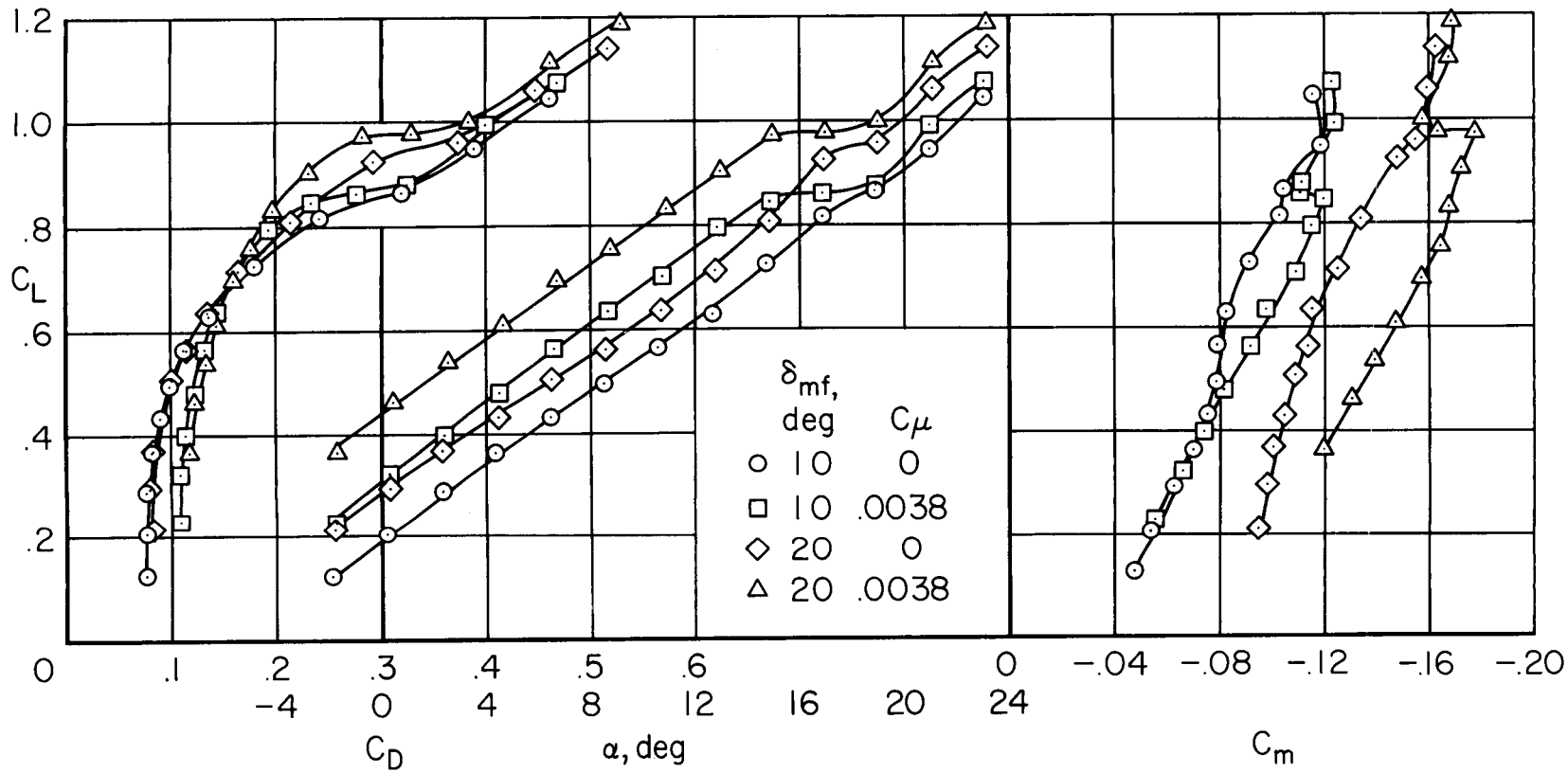

(d) $\delta_{mf} = 60^\circ$.

Figure 5.- Concluded.

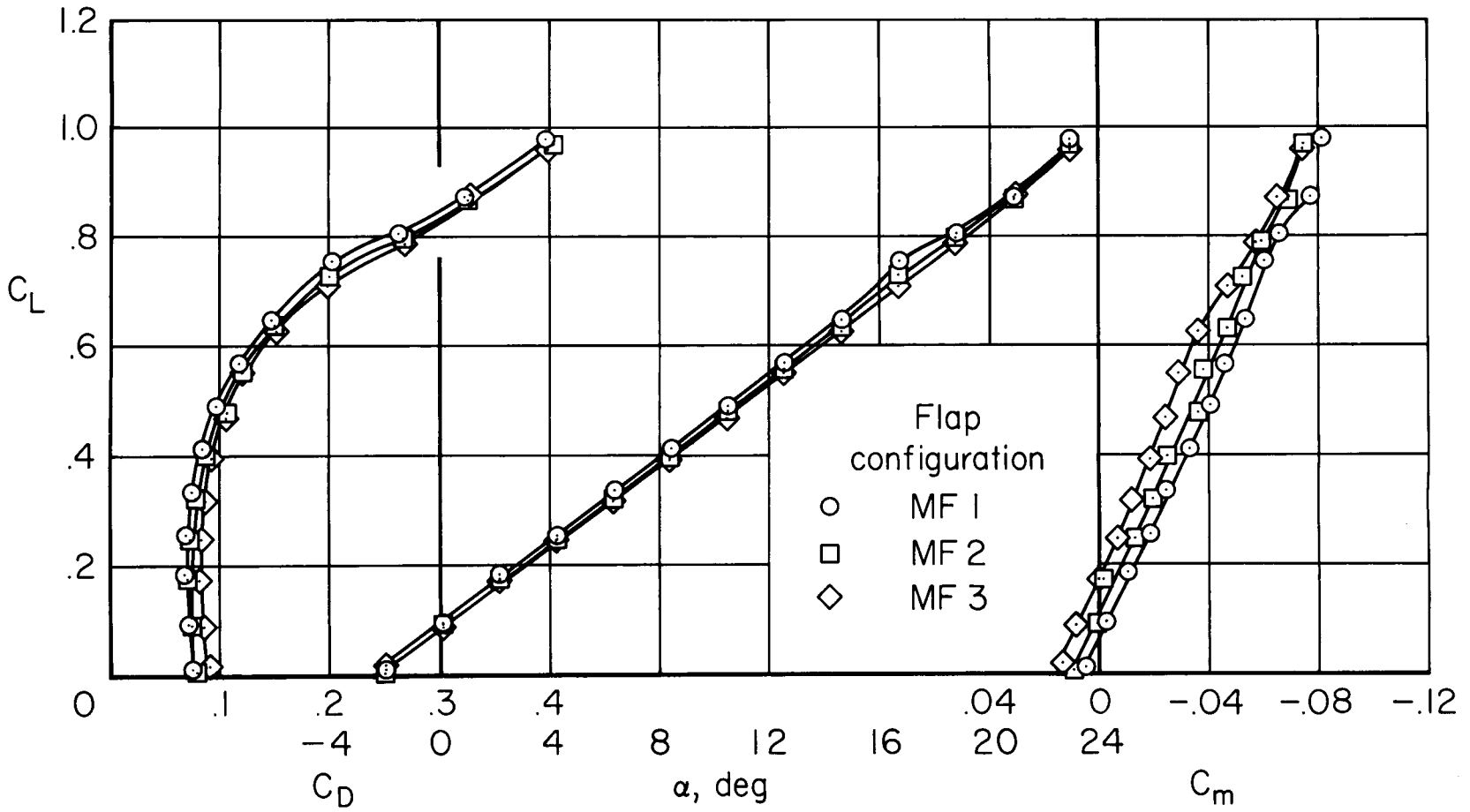

(a) $\delta_{mf} = 45^{\circ}$; BLC off.

Figure 6.- The effect of blunting the midchord flap trailing edge and wing lip on the characteristics of the model; $\delta_n = 45^{\circ}$, $c_f/c = 0.15$, $\delta_f = 0^{\circ}$.

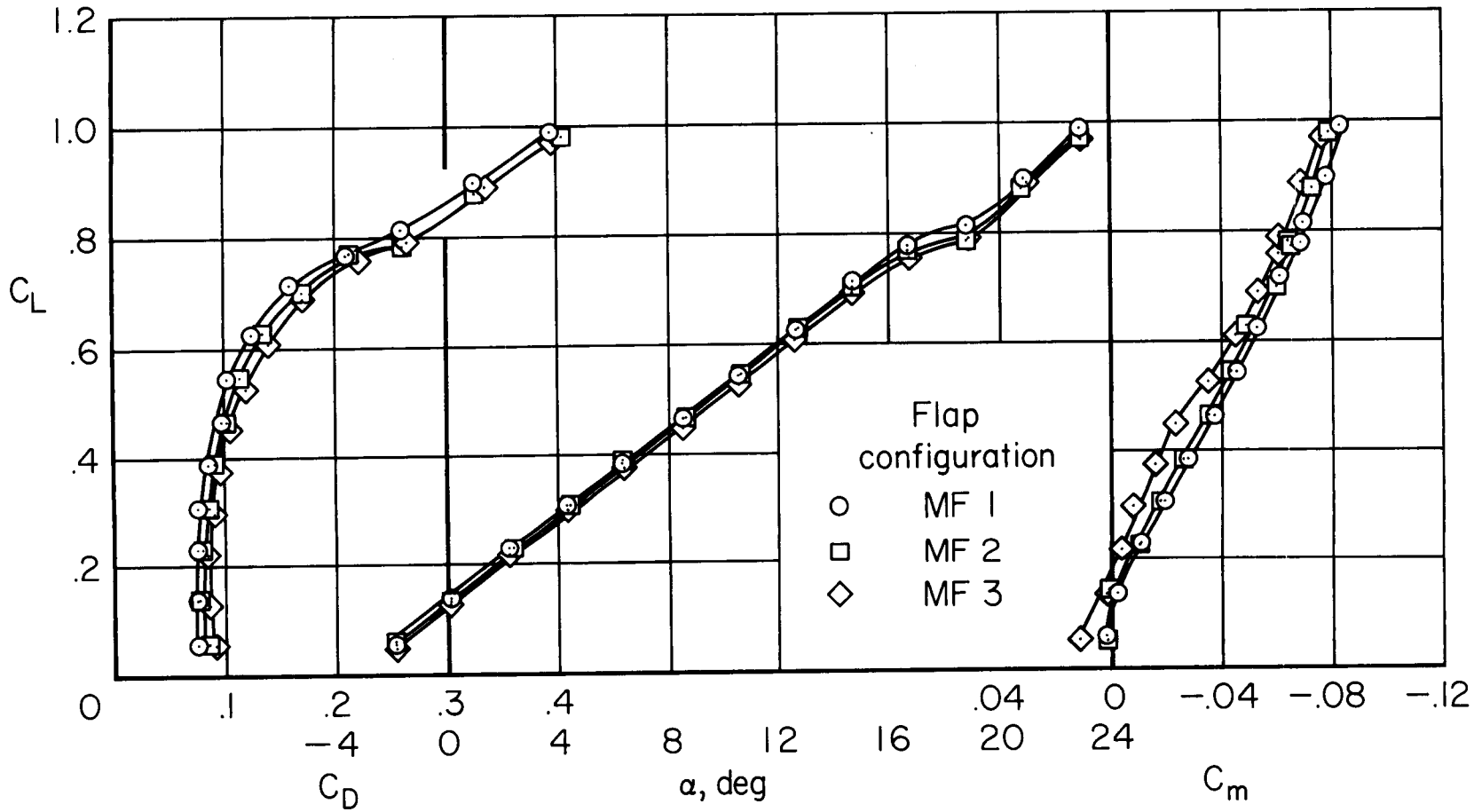

(b) $\delta_{mf} = 45°$; $C_\mu = .0.0016$.

Figure 6.- Continued.

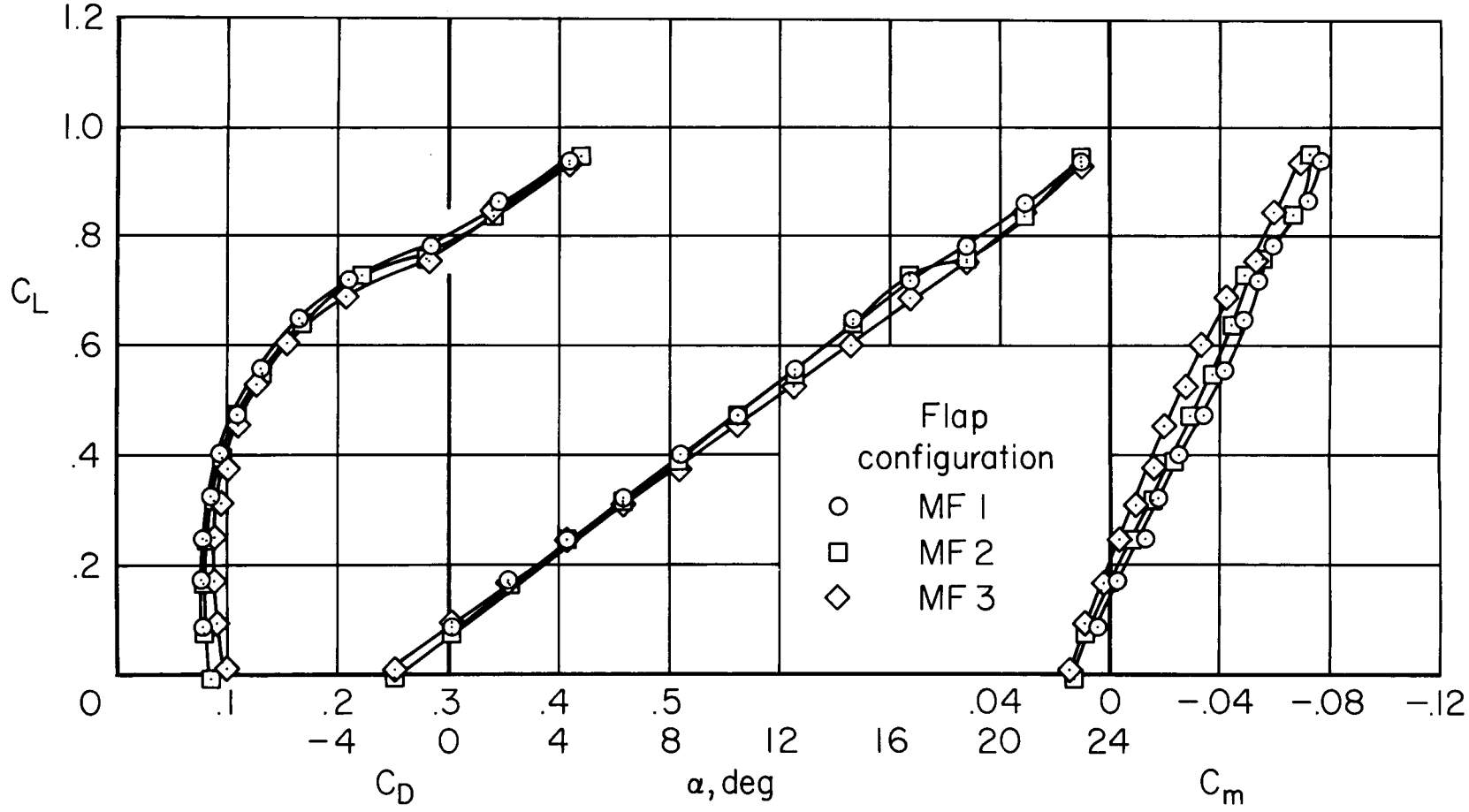

(c) $\delta_{mf} = 60^{o}$; BLC off.

Figure 6.- Continued.

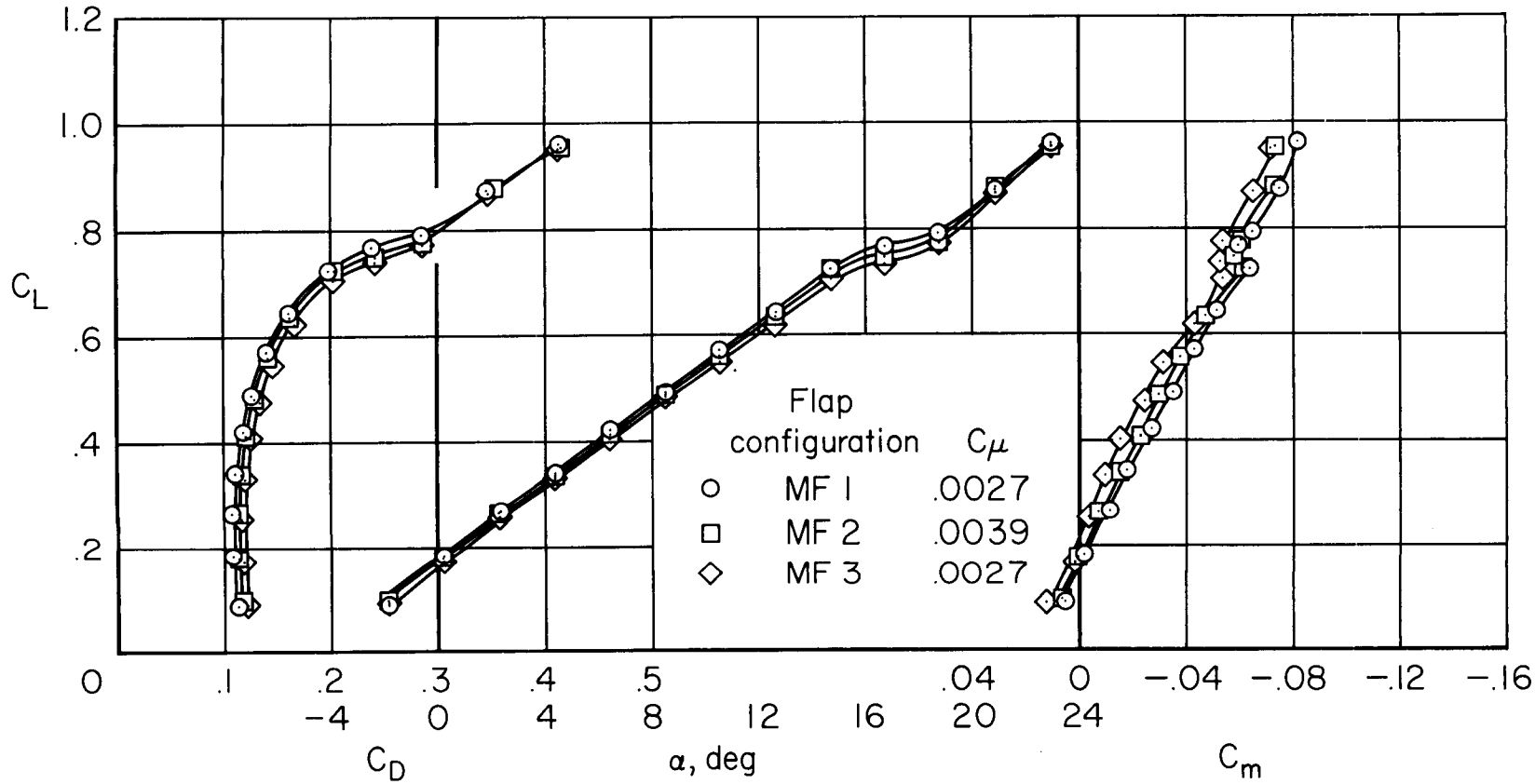

(d) $\delta_{mf} = 60^\circ$; BLC on.

Figure 6.- Concluded.

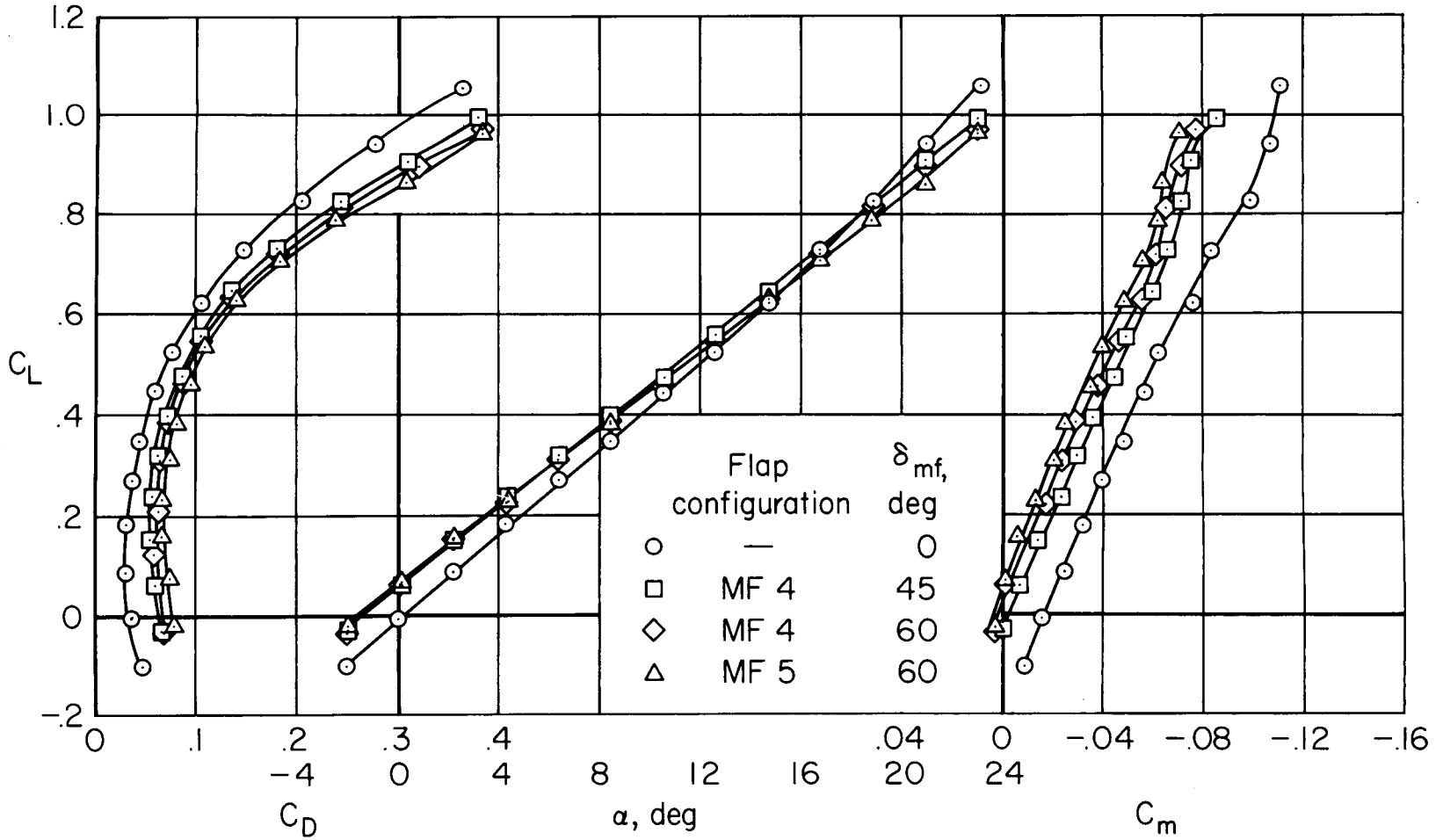

(a) BLC off.

Figure 7.- Characteristics of the model with the 10-percent chord midchord flap; $\delta_n = 45^\circ$, $\delta_f = 0^\circ$, $c_f/c = 0.10$.

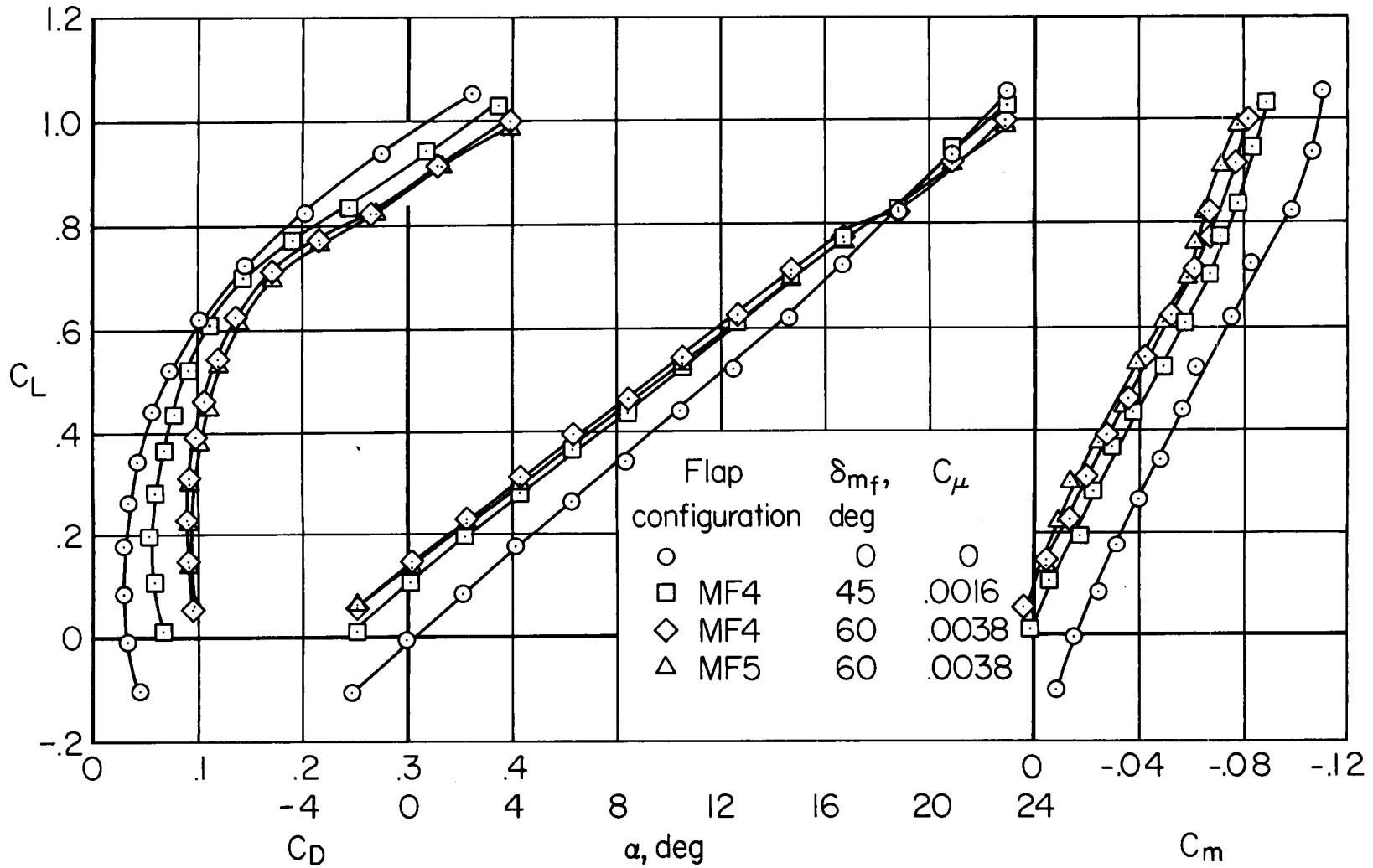

(b) BLC on.

Figure 7.- Concluded.

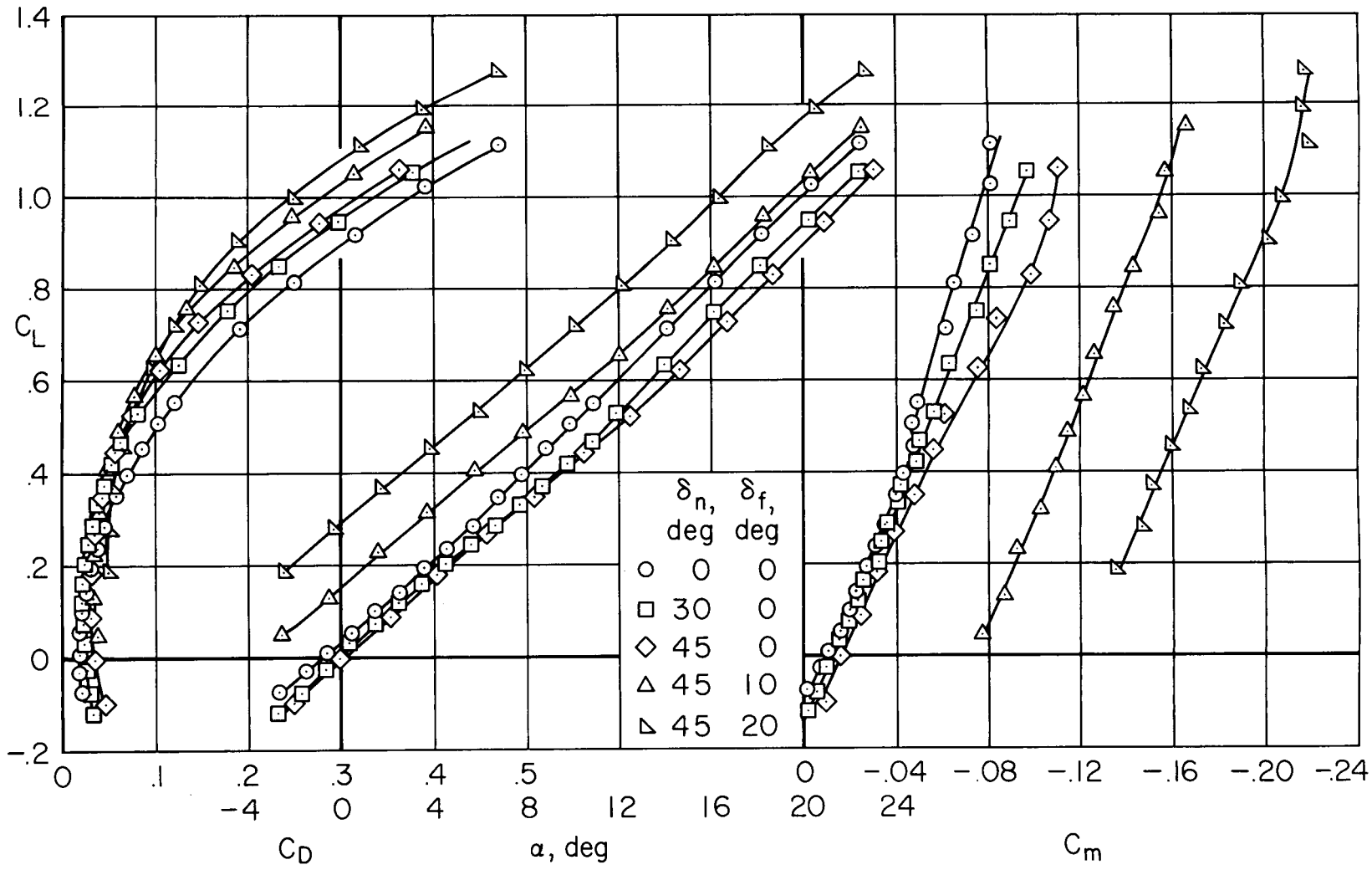

(a) $\delta_f = 0^\circ$, 10°, and 20°.

Figure 8.- Characteristics of the model with the midchord flap undeflected; $\delta_{mf} = 0^\circ$.

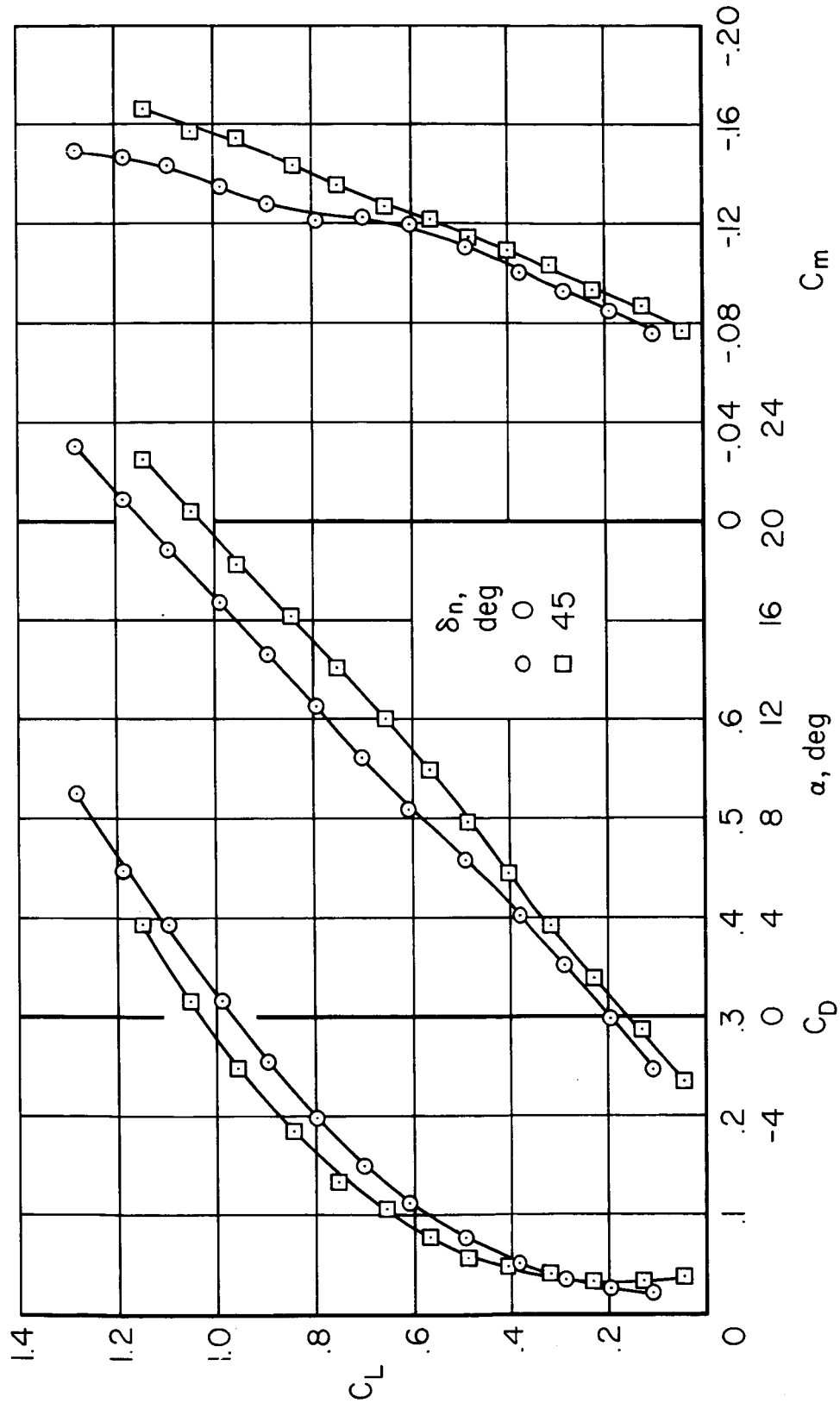

(b) Effect of LE flap with $\delta_f = 10^\circ$.

Figure 8.- Concluded.

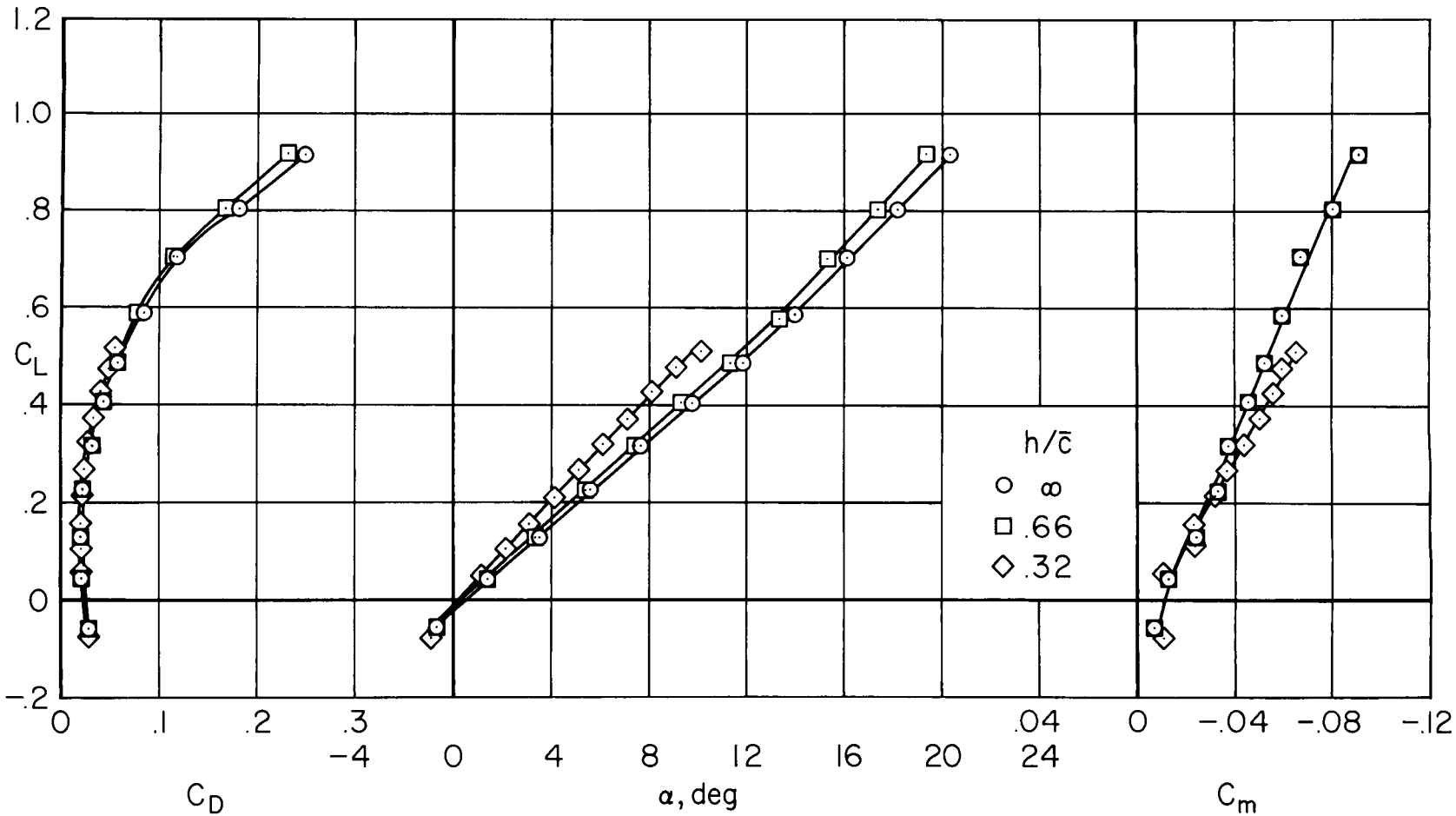

(a) $\delta_{mf} = 0^{o}$; $\delta_f = 0^{o}$, ground-plane system.

Figure 9.- Characteristics of the model in the presence of the ground; $\delta_n = 45^{o}$, MF 4($c_f/c = 0.10$).

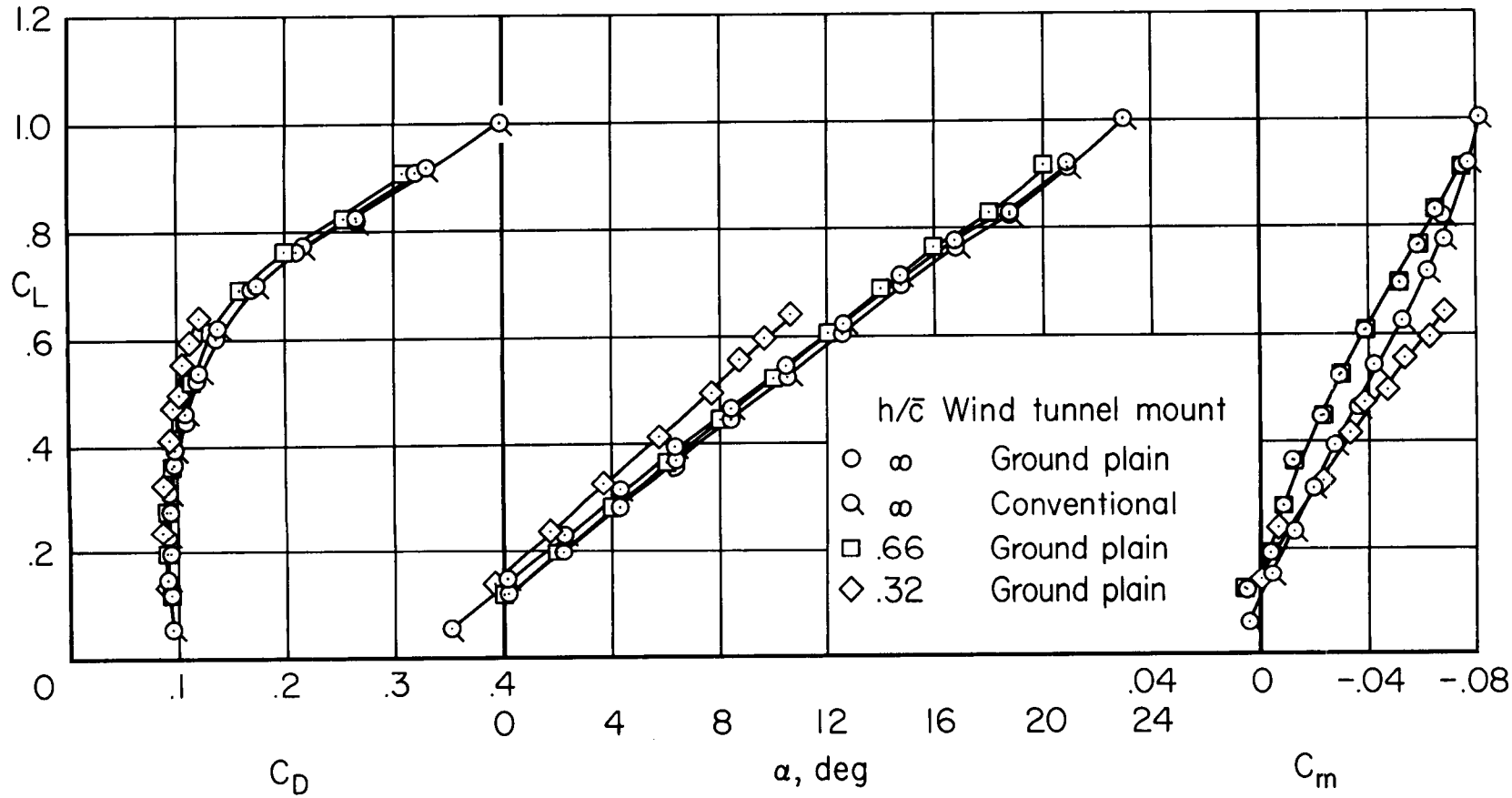

(b) $\delta_{mf} = 60^{\circ}$; $C_{\mu} = 0.0038$, $\delta_f = 0^{\circ}$.

Figure 9.- Continued.

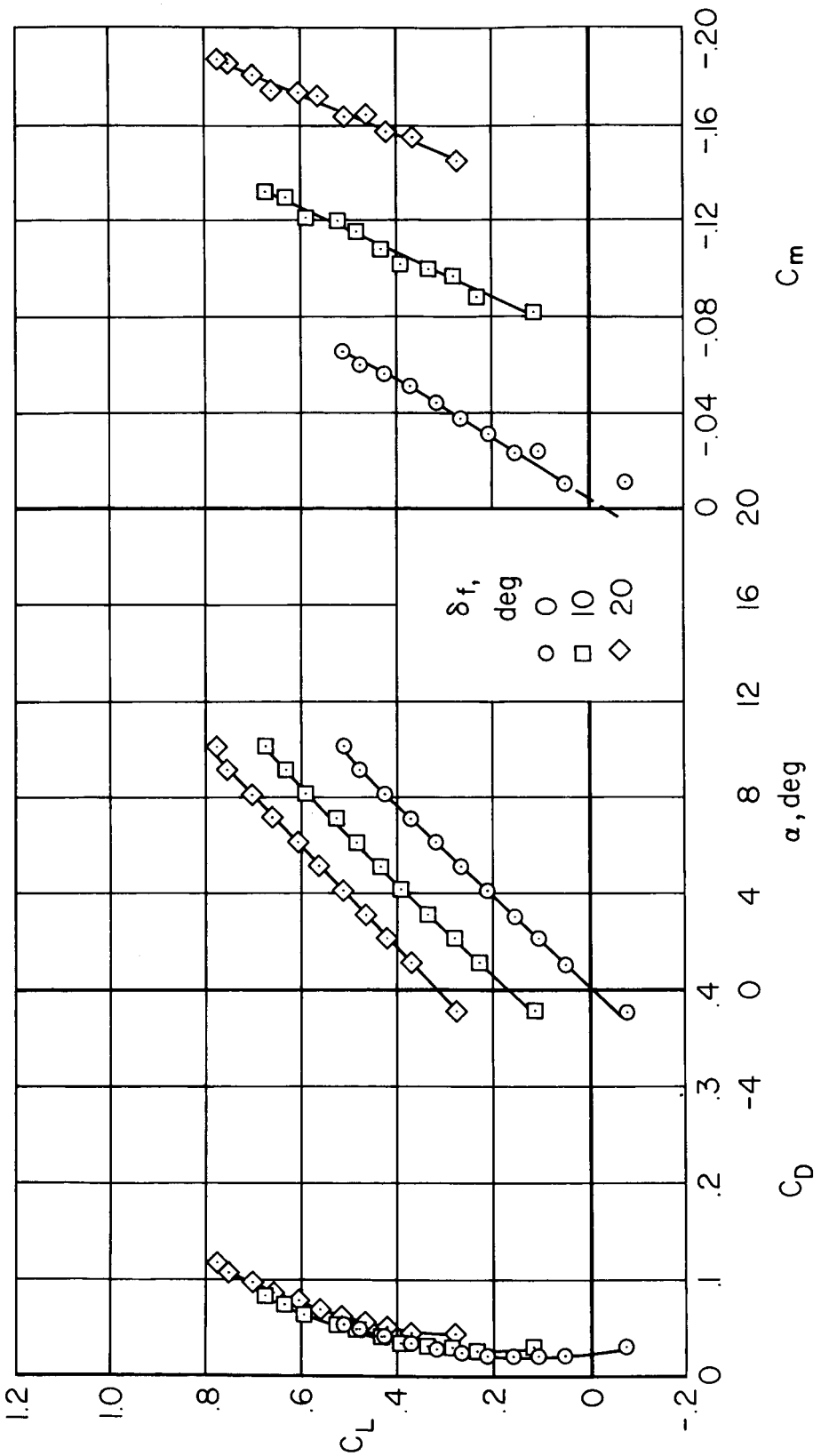

(c) $\delta_{mf} = 0^{\circ}$; $h/\bar{c} = 0.32$, ground-plane system.

Figure 9.- Continued.

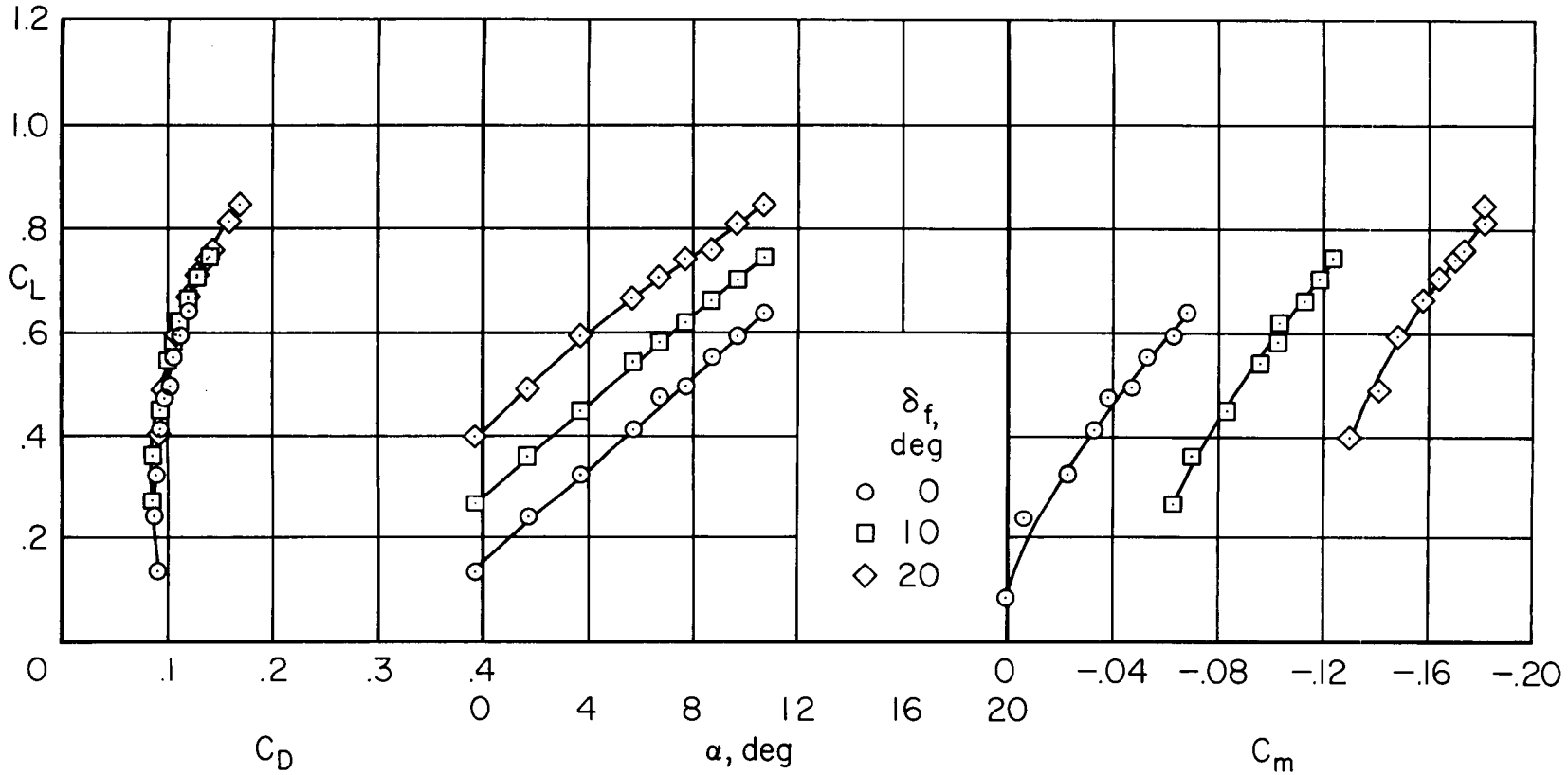

(d) $\delta_{mf} = 60°$; $C_\mu = 0.0038$, $h/\bar{c} = 0.32$, ground-plane system.

Figure 9.- Concluded.

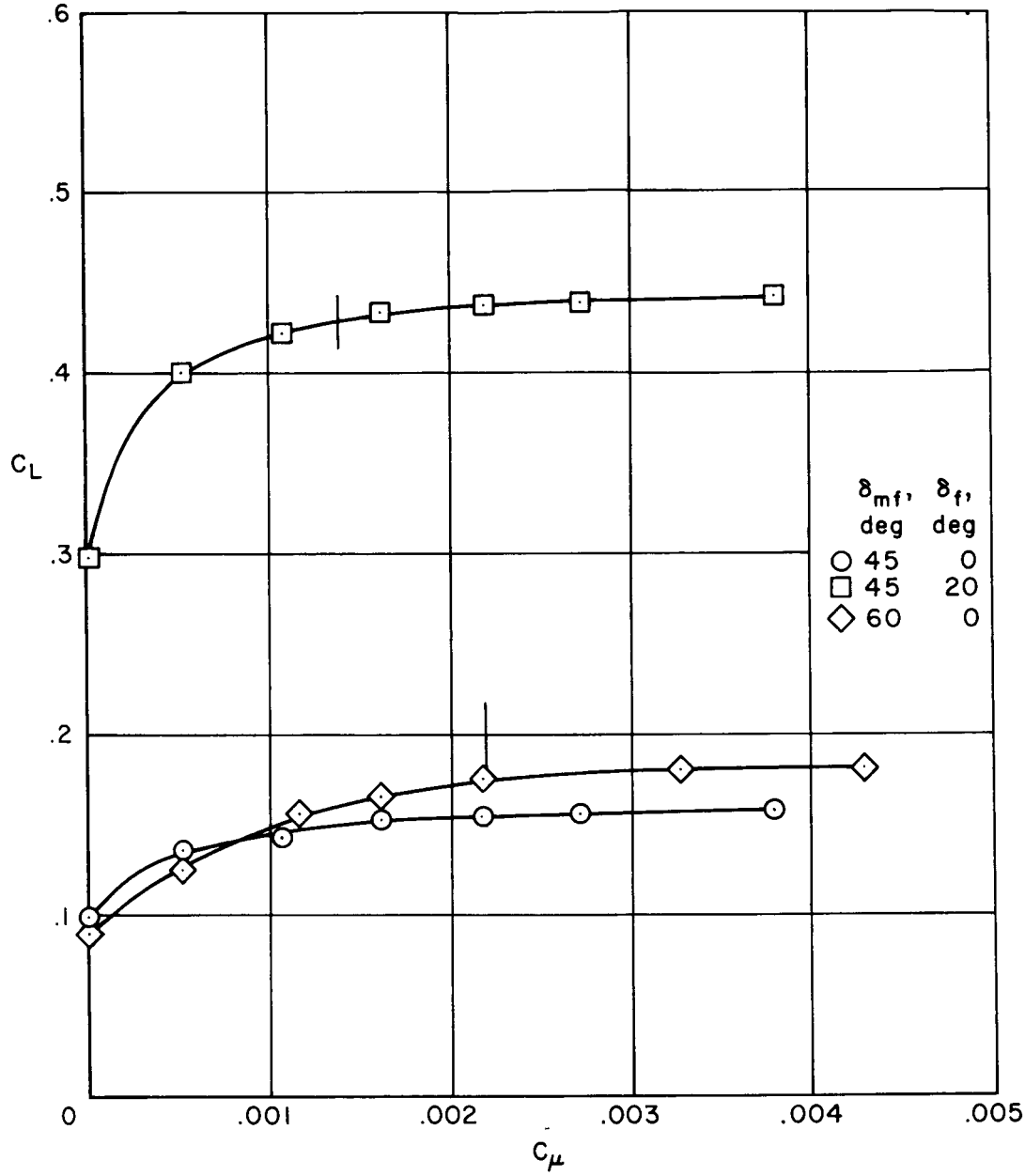

(a) MF 1(c_f/c = 0.15); $\alpha = 0^\circ$.

Figure 10.- Variation of C_L with C_μ; $\delta_n = 45^\circ$.

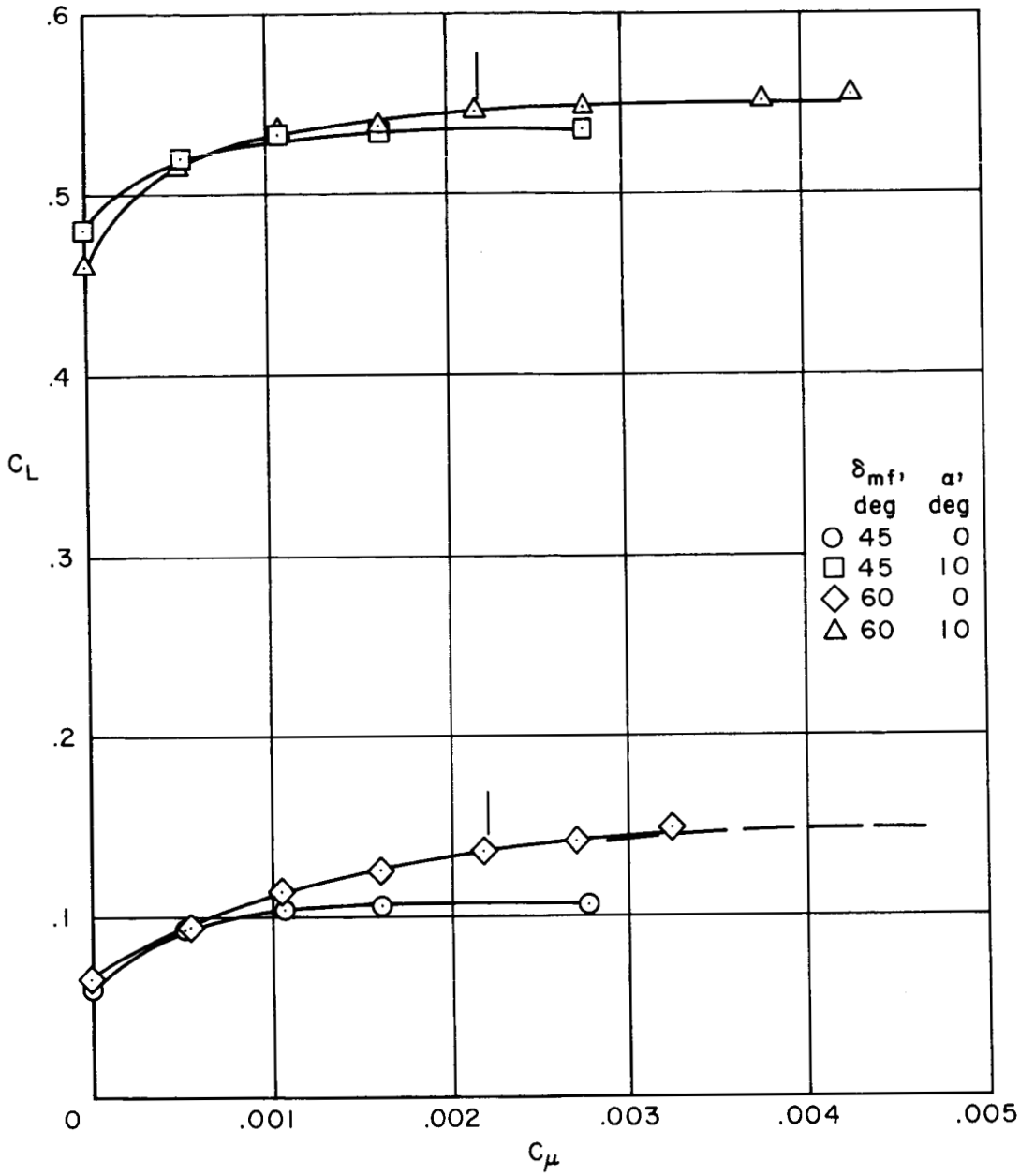

(b) MF 4(c_f/c = 0.10); $\delta_f = 0^\circ$.

Figure 10.- Concluded.

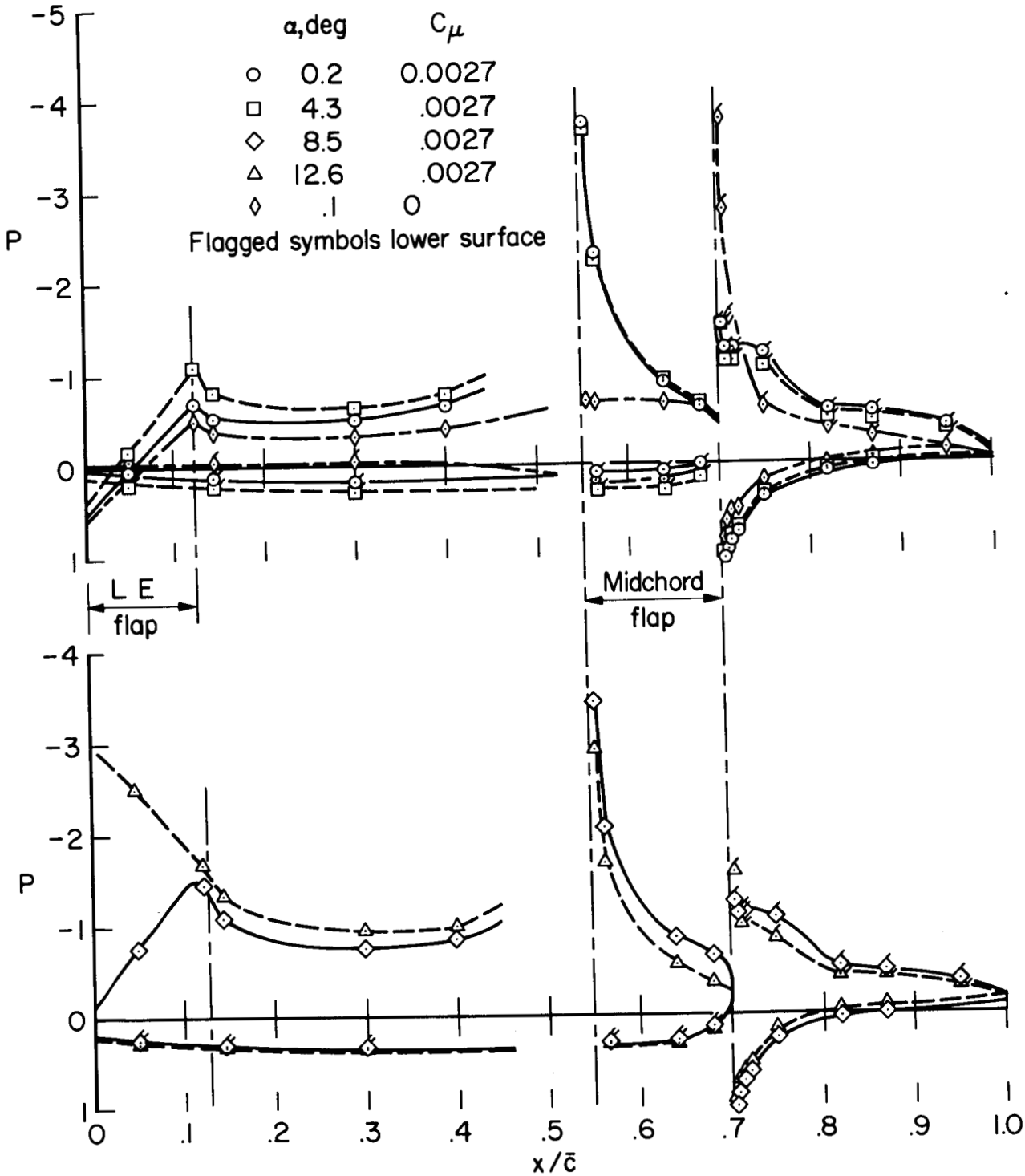

(a) $\delta_f = 0^\circ$.

Figure 11.- Chordwise pressure distribution at the 50-percent span station with the midchord flap deflected to $\delta_{mf} = 60^\circ$; $\delta_n = 45^\circ$, MF 1($c_f/c = 0.15$).

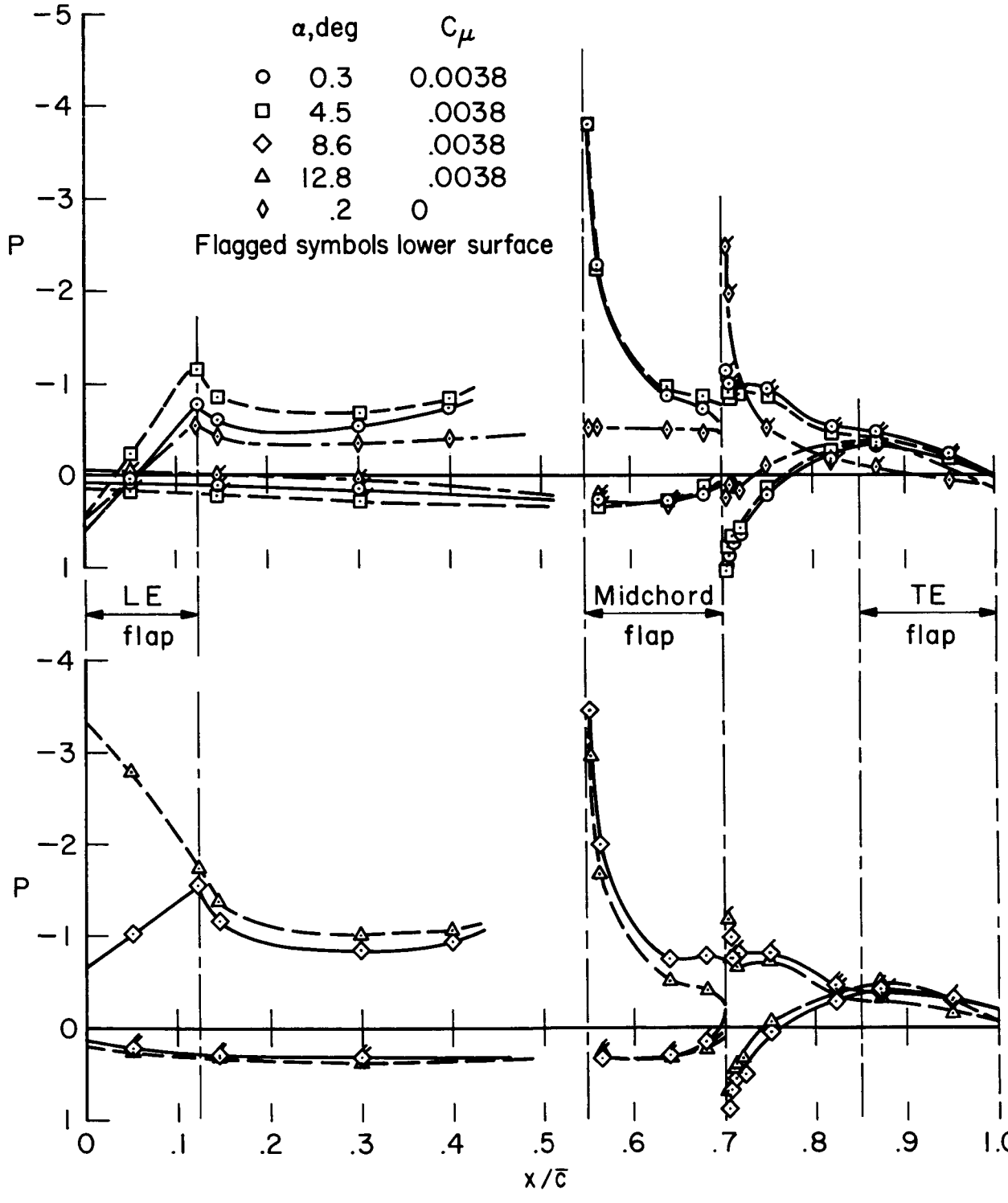

(b) $\delta_f = 10^\circ$.

Figure 11.- Continued.

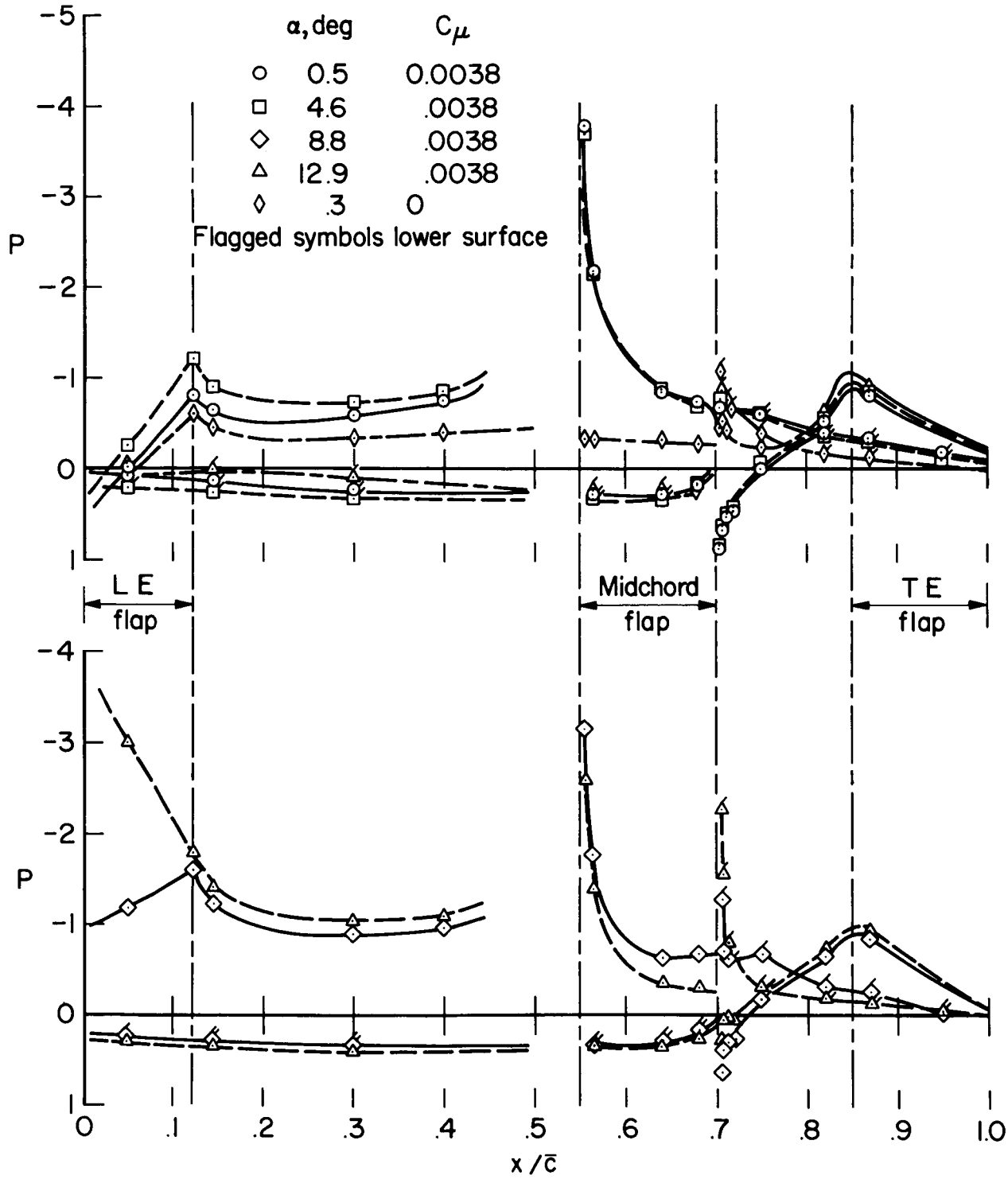

(c) $\delta_f = 20^\circ$.

Figure 11.- Concluded.

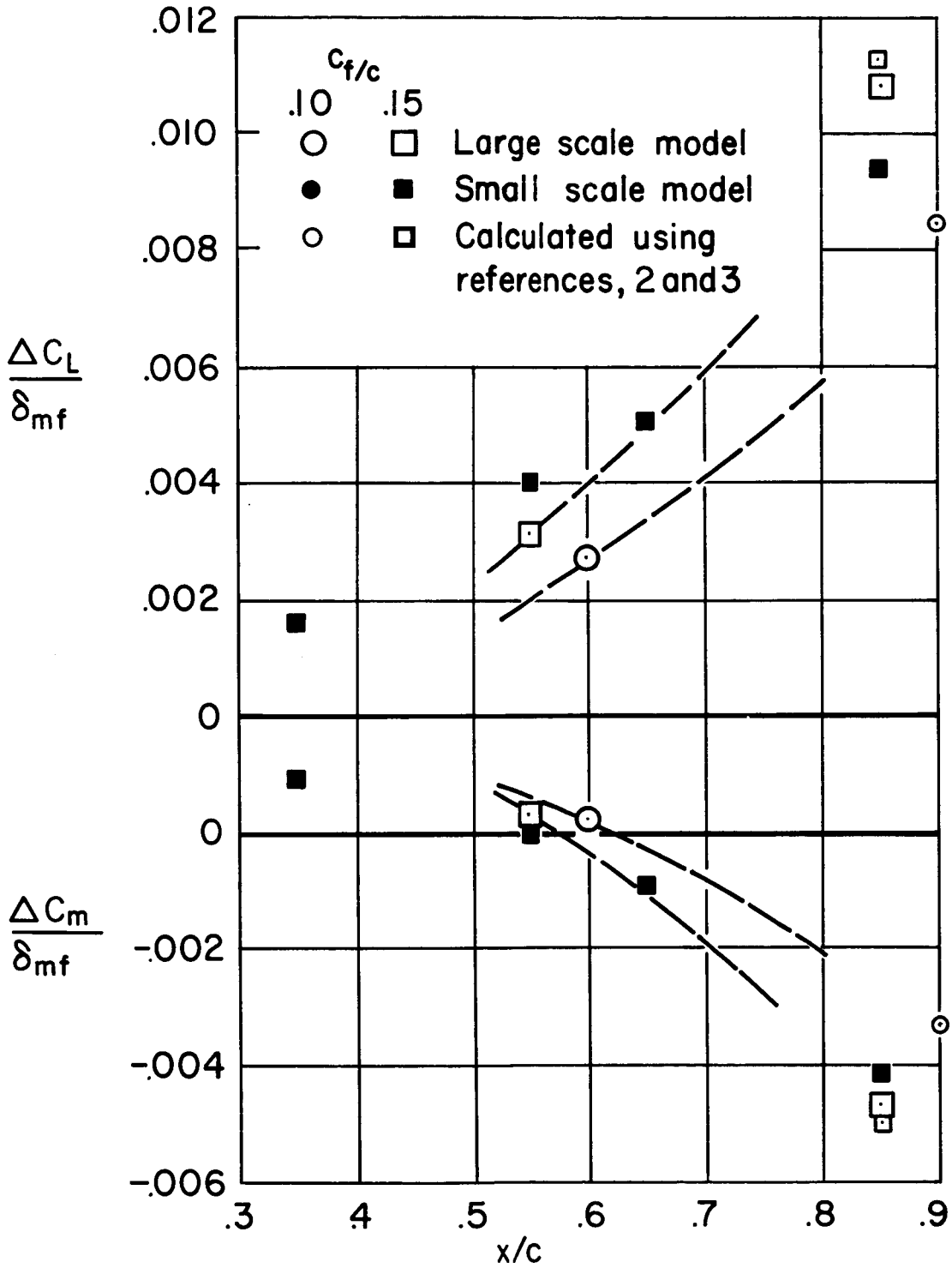

Figure 12.- The variation with flap chordwise position of the lift and pitching-moment increments due to flap deflection; $\delta_{mf} = 45^{\circ}$, BLC on for the midchord flaps, $\delta_f = 20^{\circ}$ for the trailing-edge flaps at $\alpha = 0^{\circ}$, $\delta_n = 45^{\circ}$.

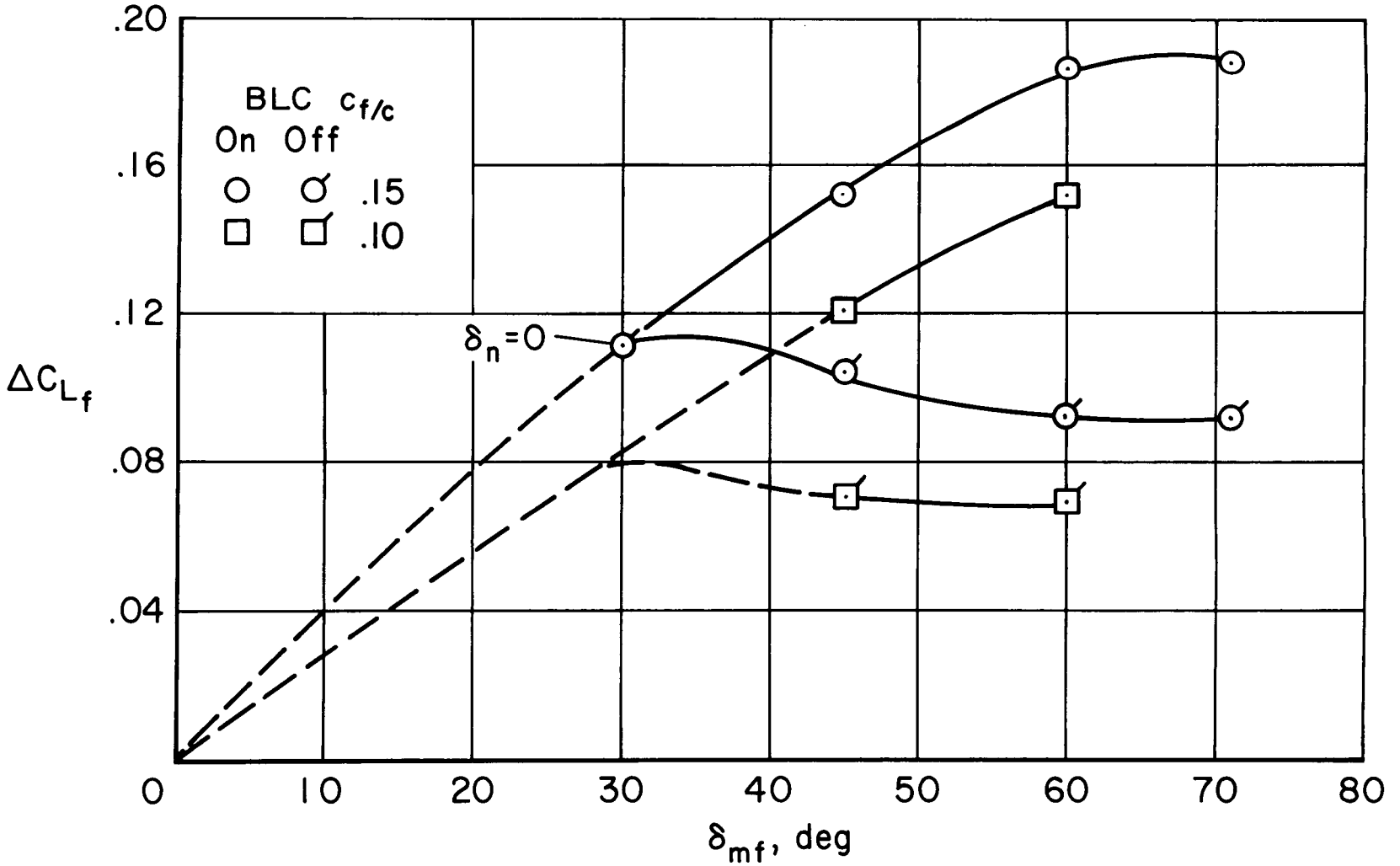

Figure 13.- The variation of midchord flap lift increment with flap deflection with and without BLC; $\alpha = 0^o$, $\delta_n = 45^o$ unless otherwise noted, $\delta_f = 0^o$, MF 1 and MF 4.

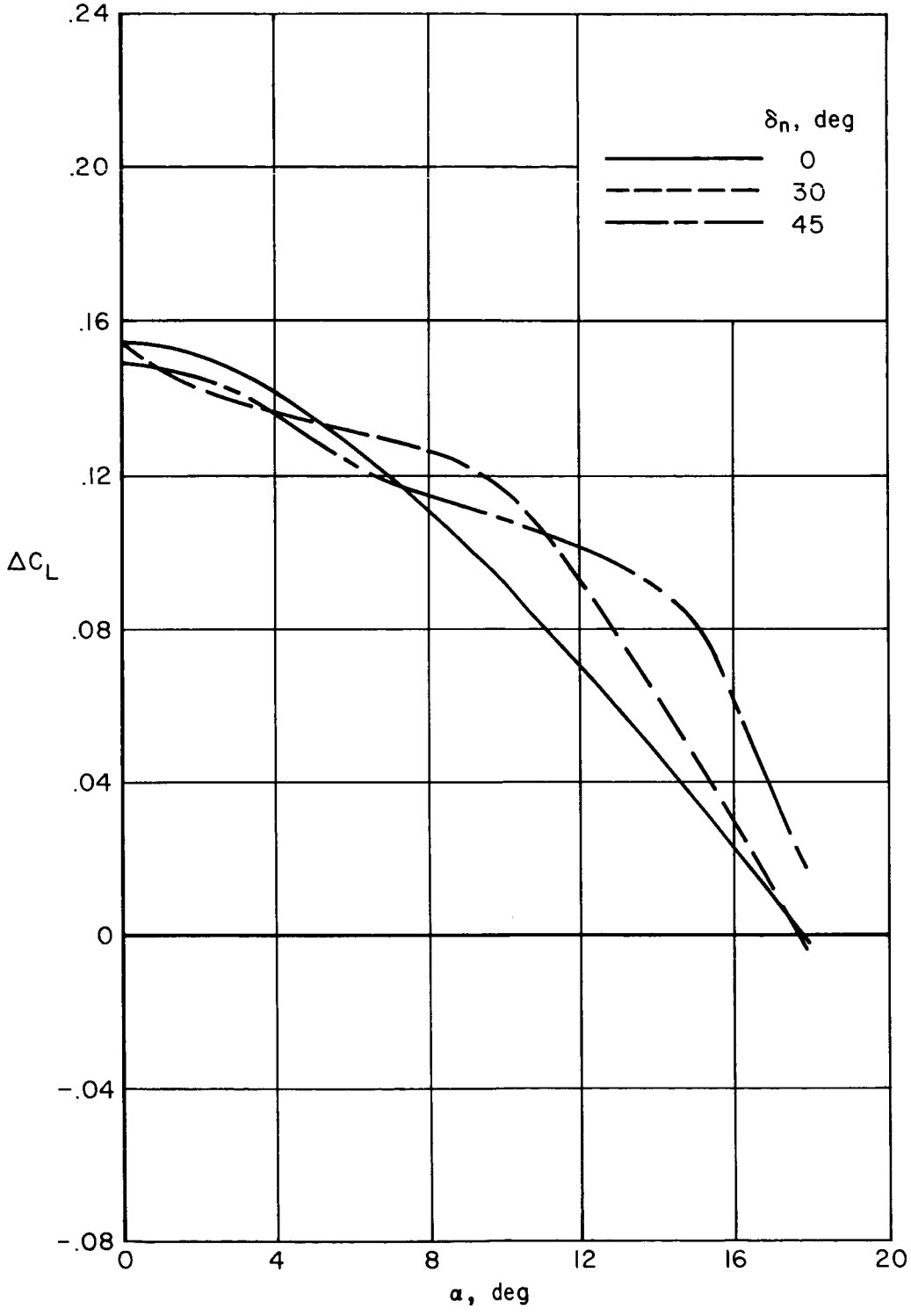

(a) $\delta_{mf} = 45^\circ$.

Figure 14.- The effect of leading-edge flap deflection on the flap lift increment of the midchord flap with BLC; $\delta_f = 0^\circ$, MF 1($c_f/c = 0.15$).

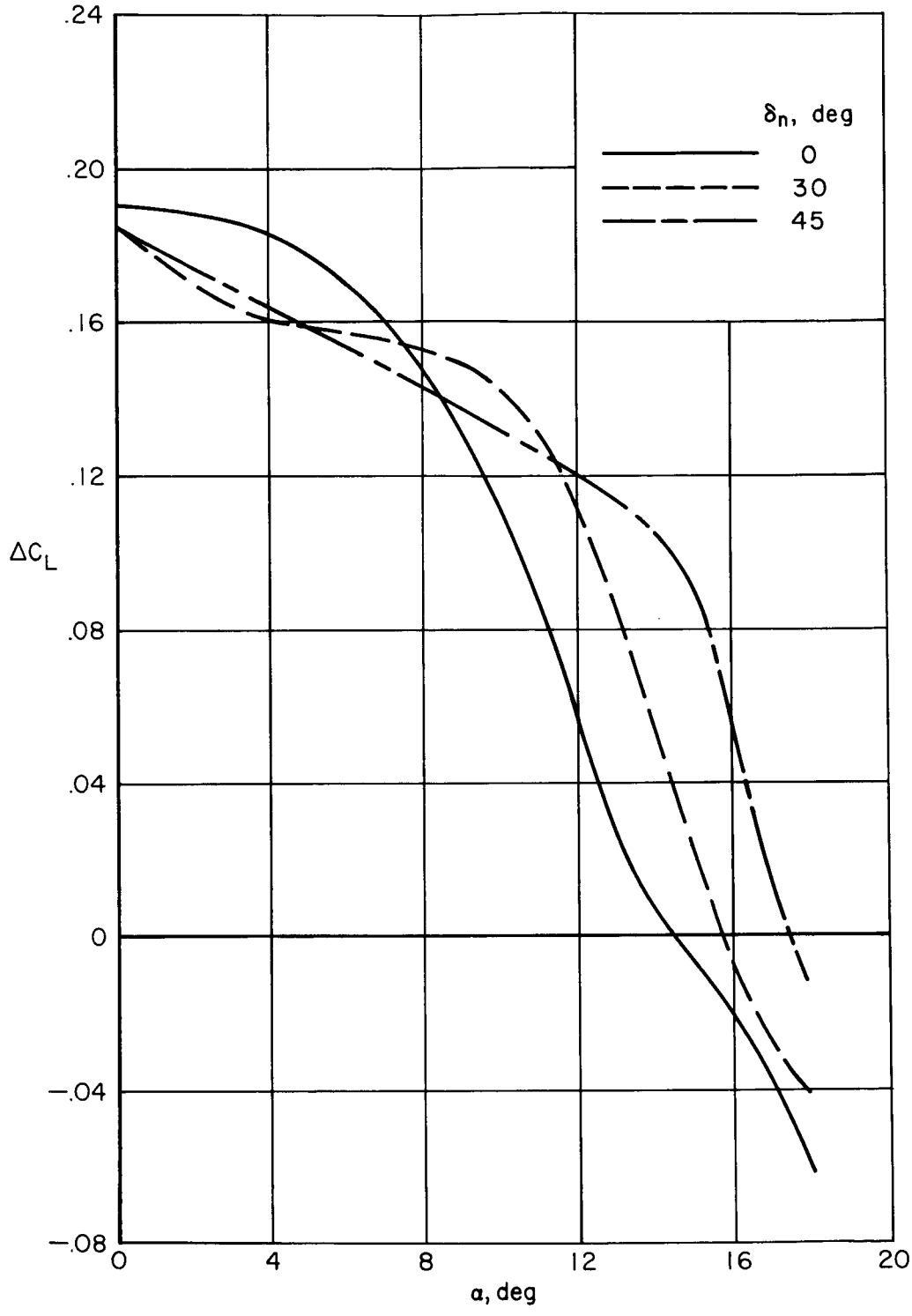

(b) $\delta_{mf} = 60°$.

Figure 14.- Concluded.

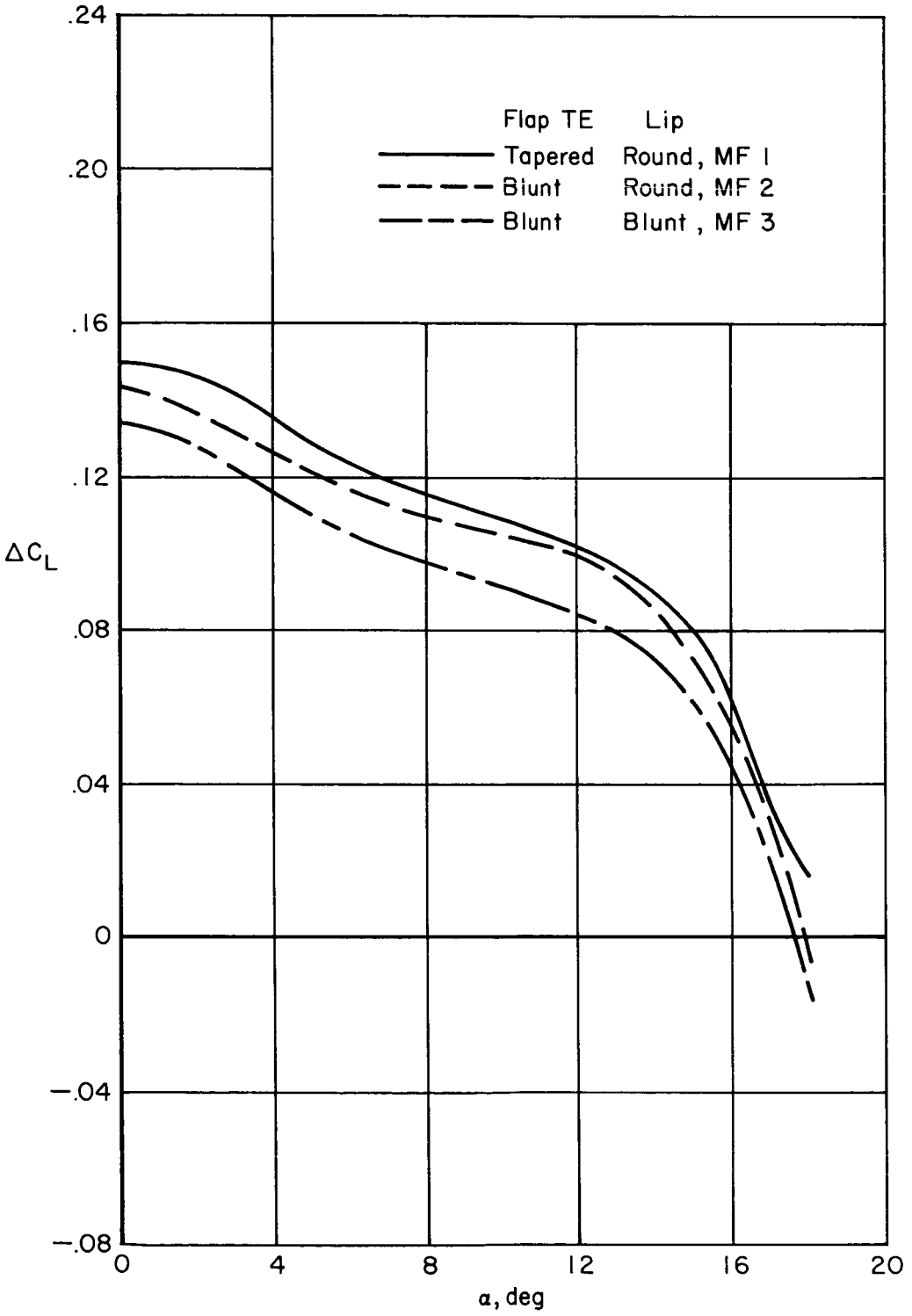

(a) $\delta_{mf} = 45^{\circ}$.

Figure 15.- The effect of blunting the midchord flap and wing lip on the midchord flap lift increment; BLC on, $\delta_n = 45^{\circ}$, $\delta_f = 0^{\circ}$, $c_f/c = 0.15$.

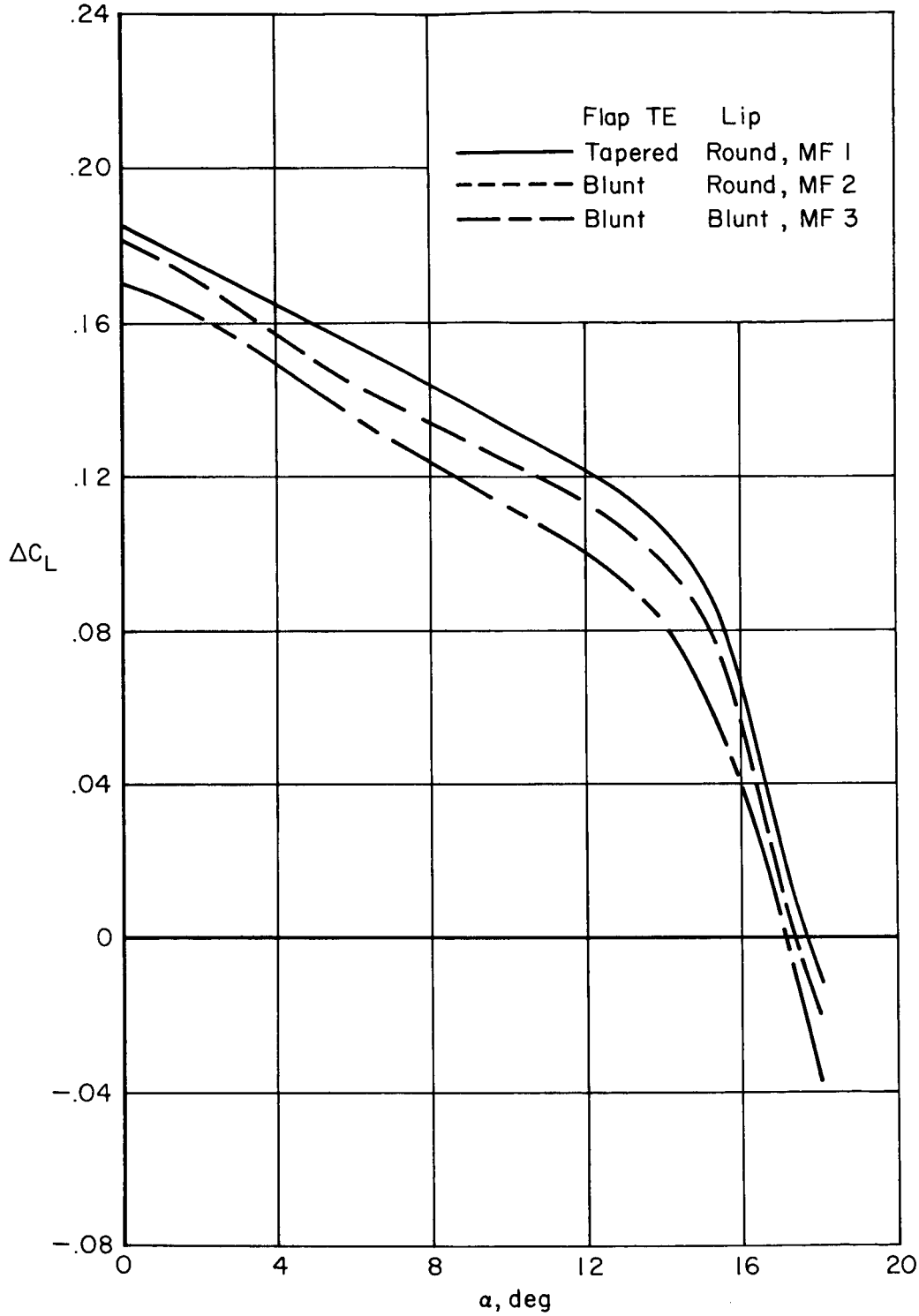

(b) $\delta_{mf} = 60^{\circ}$.

Figure 15.- Concluded.

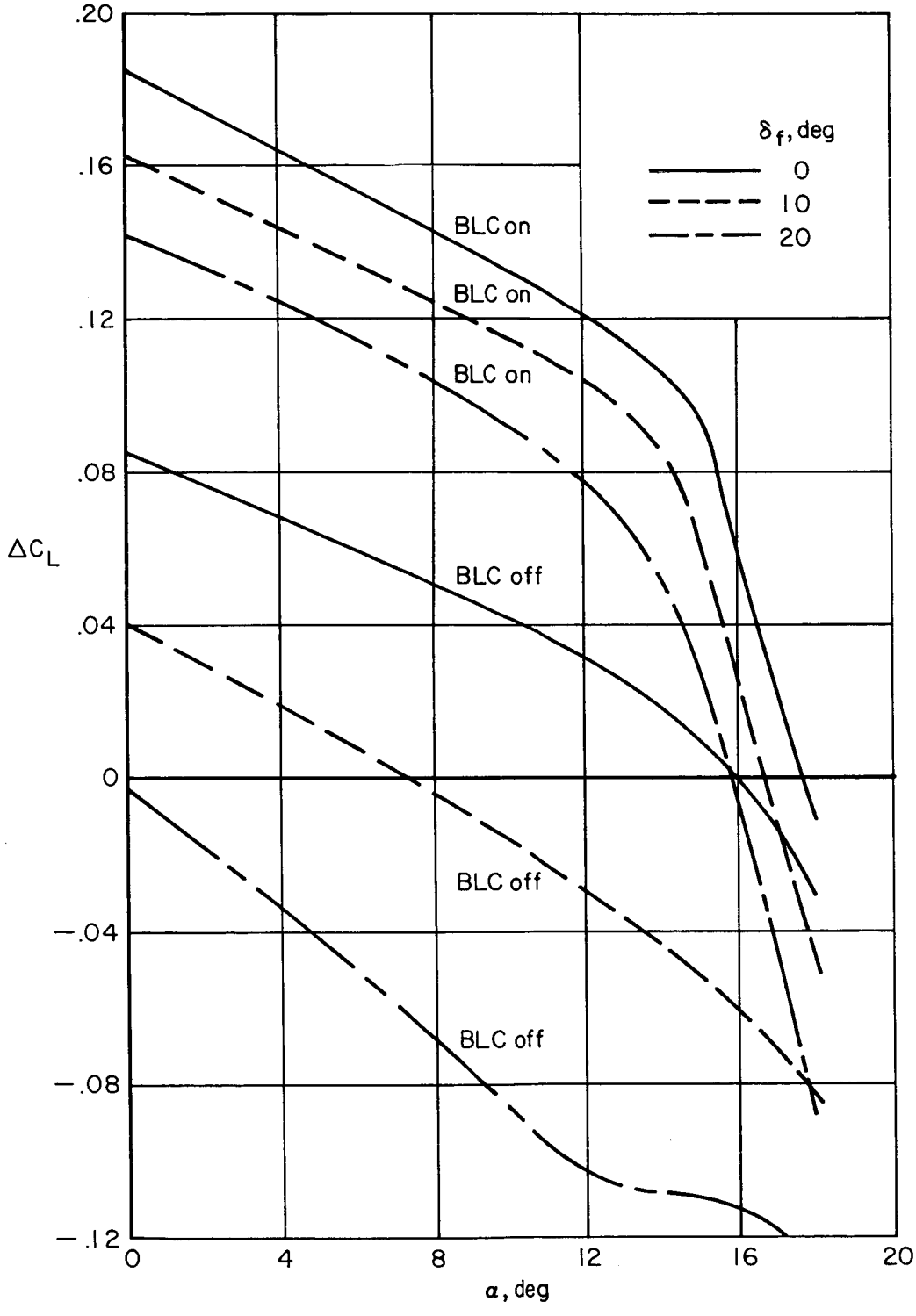

Figure 16.- The effect of trailing-edge flap deflection on the midchord flap lift increment with and without BLC; $\delta_n = 45°$, $\delta_{mf} = 60°$, MF 1($c_f/c = 0.15$).

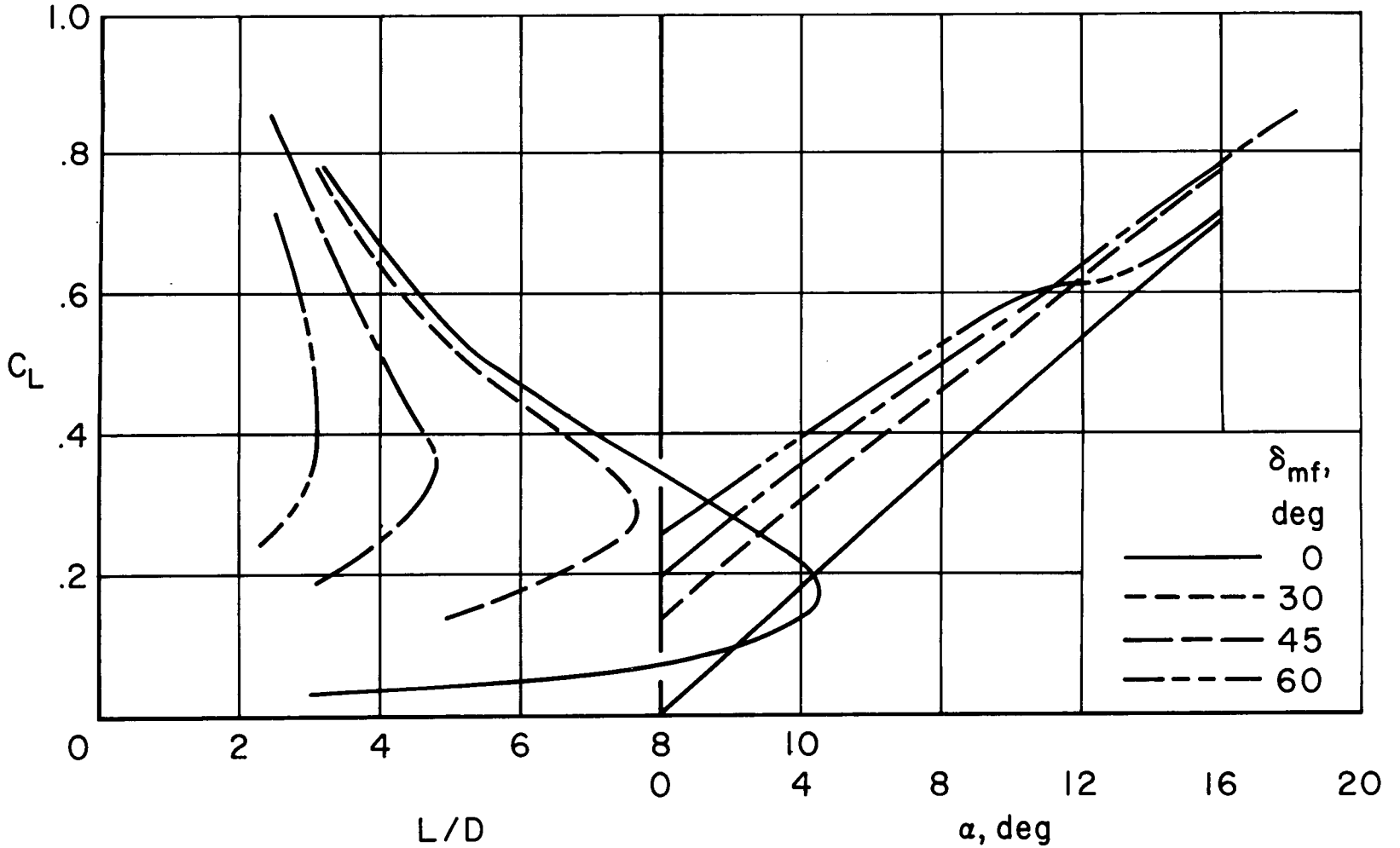

(a) $\delta_n = 0^o$.

Figure 17.- Characteristics of the model trimmed for a static margin of 4 percent by means of the trailing-edge flaps used as elevons; MF 1(c_f/c = 0.15), HLC on, C_{D_o} = 0.0100 (flaps undeflected).

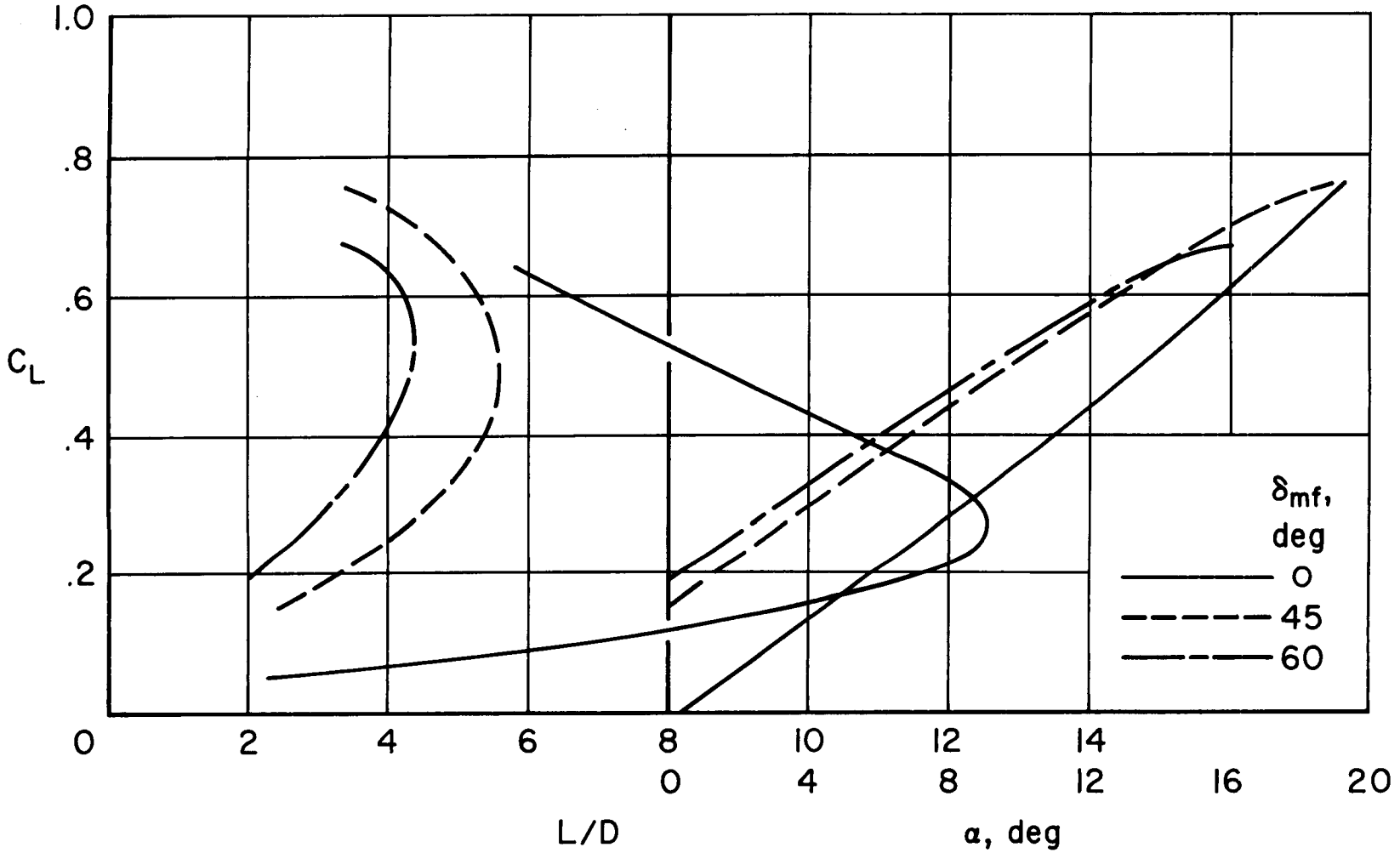

(b) $\delta_n = 45°$.

Figure 17.- Concluded.

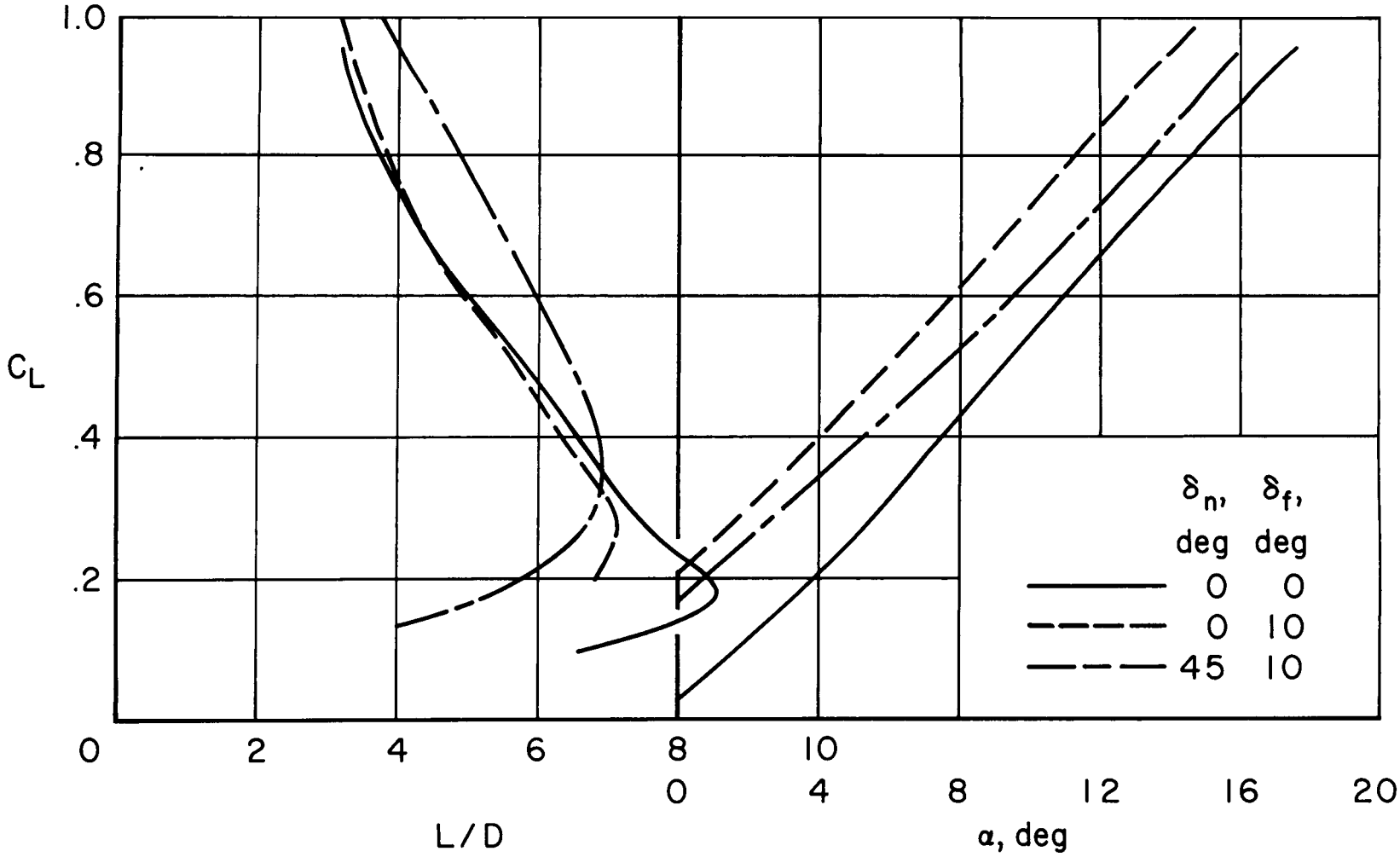

(a) $\delta_{mf} = 0^\circ$.

Figure 18.- Characteristics of the model trimmed for static margins between 1 and 3 percent by means of a canard control; MF 1(0.15), BLC on for $\delta_{mf} = 45^\circ$ and 60°, $C_{D_o} = 0.0100$ (flaps undeflected).

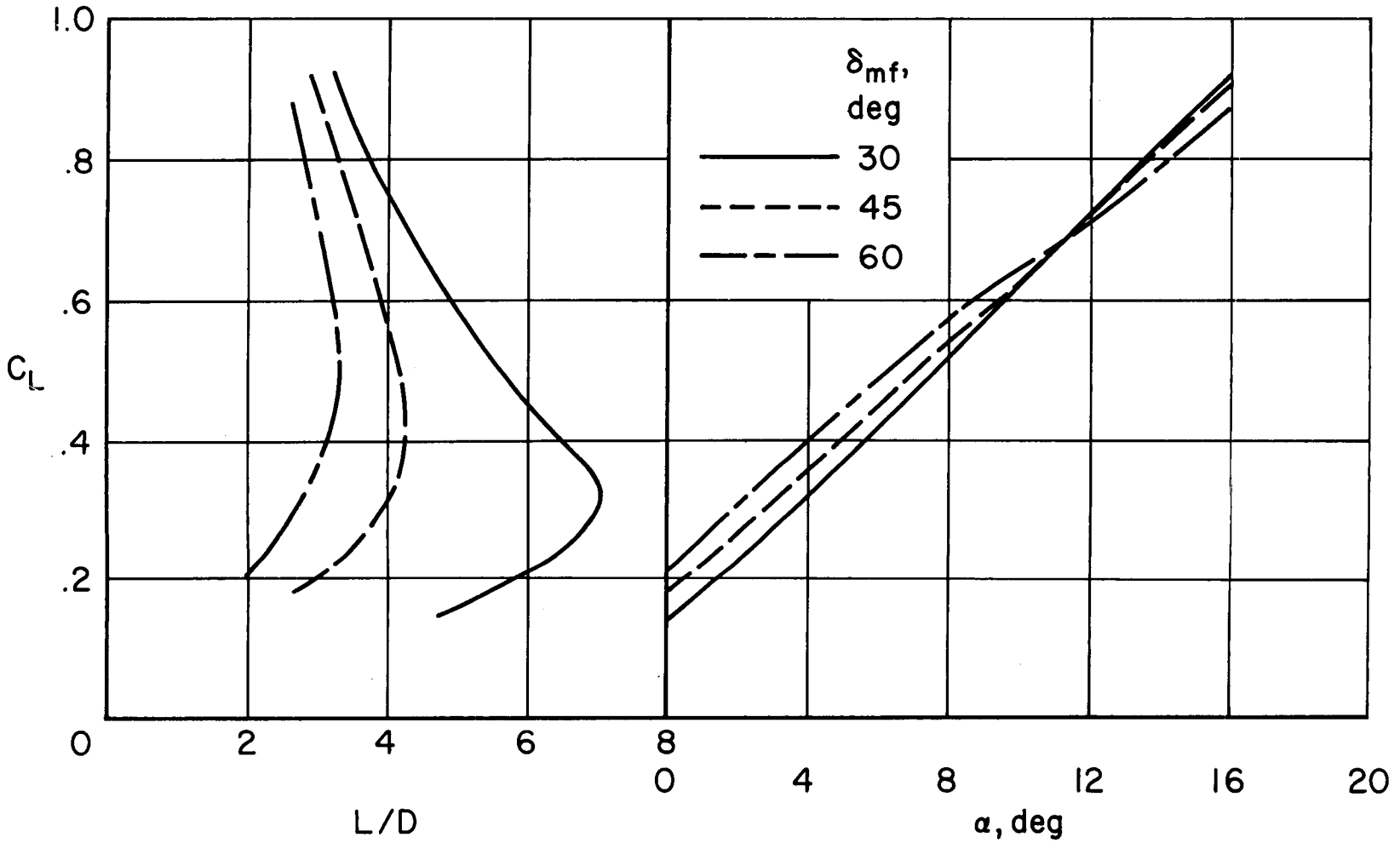

(b) $\delta_n = 0^o$; $\delta_f = 0^o$.

Figure 18.- Continued.

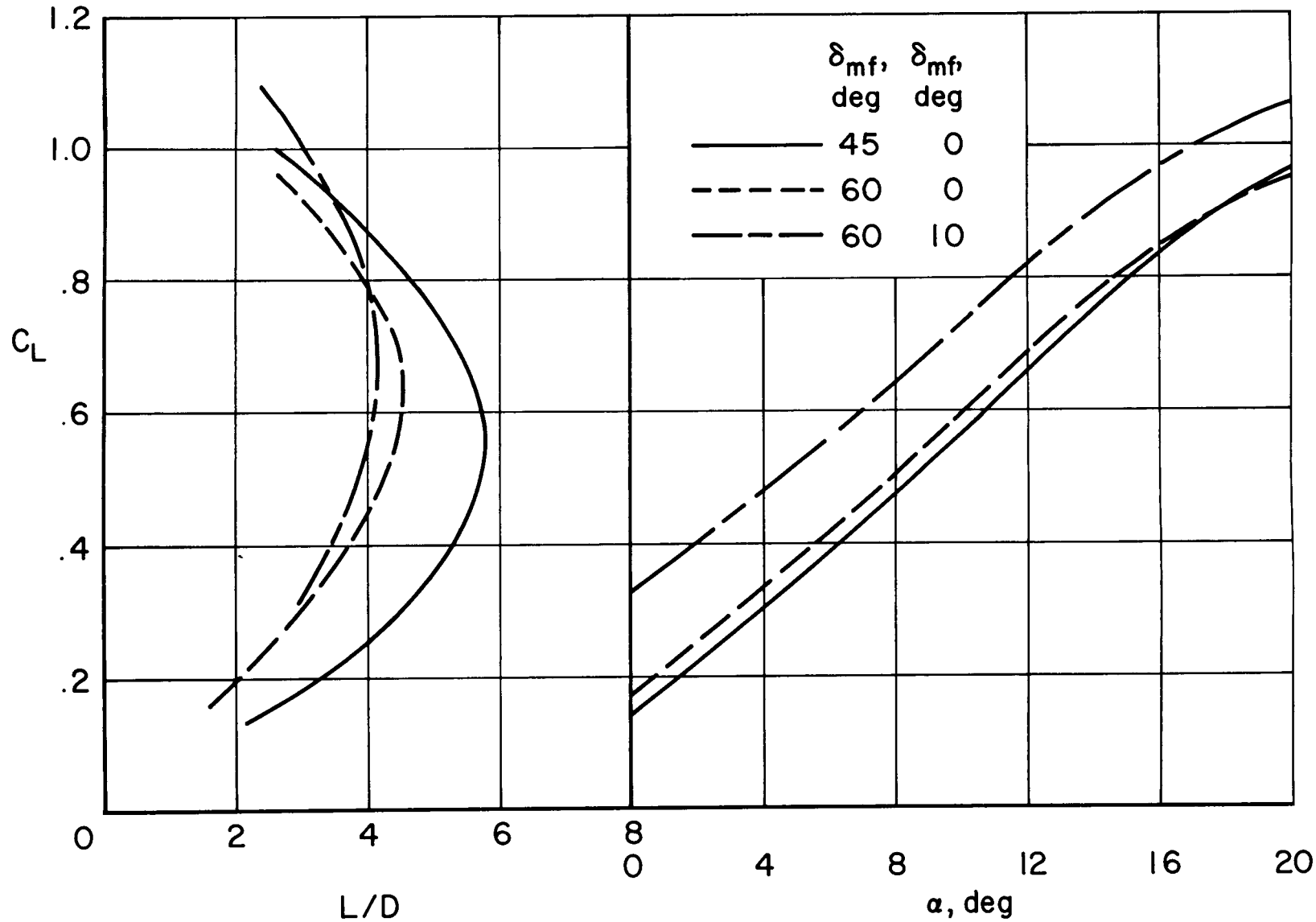

(c) $\delta_n = 45°$.

Figure 18.- Concluded.

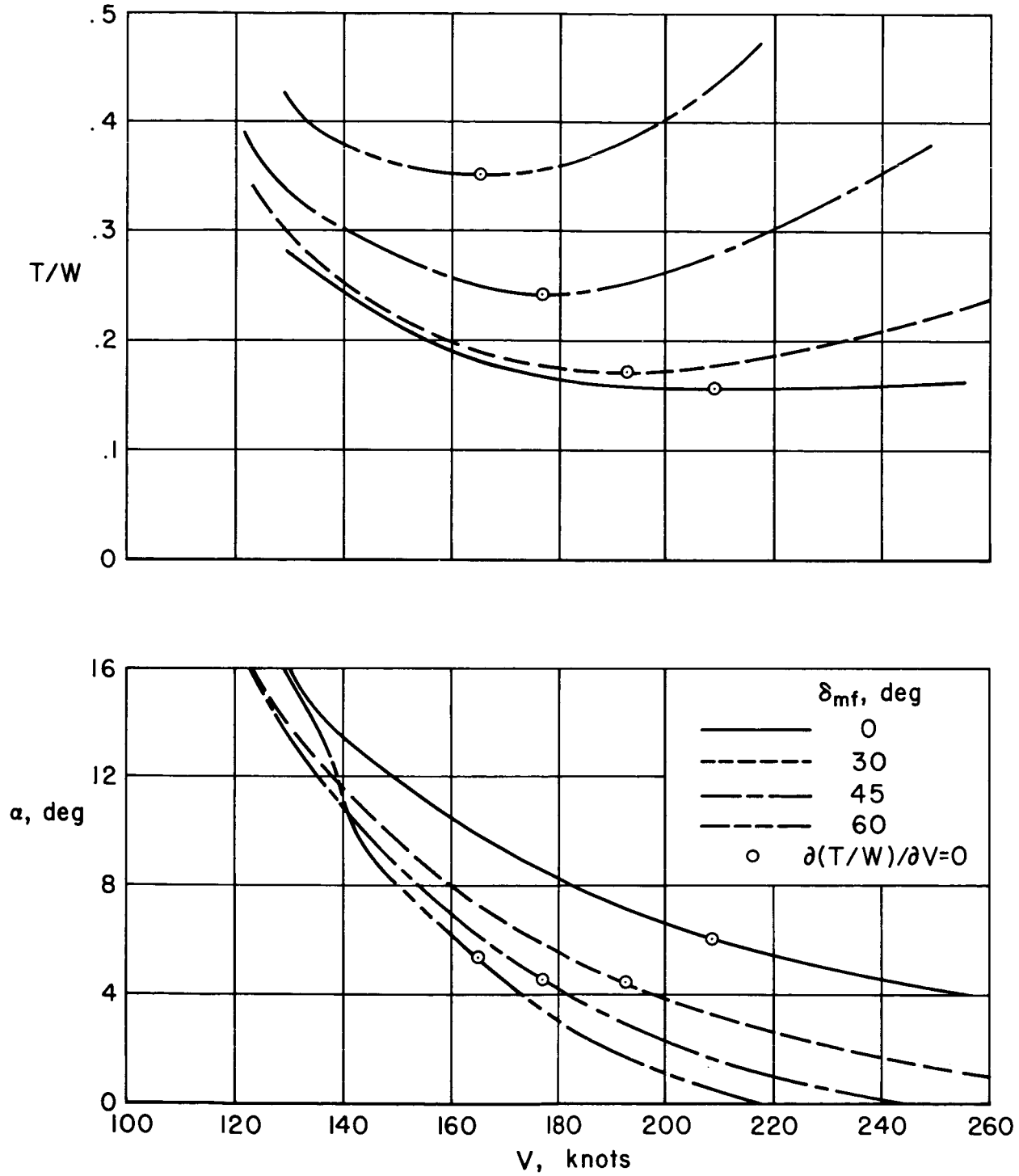

(a) $\delta_n = 0^o$.

Figure 19.- The variations of thrust-to-weight ratio and angle of attack with airspeed for the model trimmed by means of the trailing-edge flaps used as elevons; W/S = 40 psf, MF 1(c_f/c = 0.15).

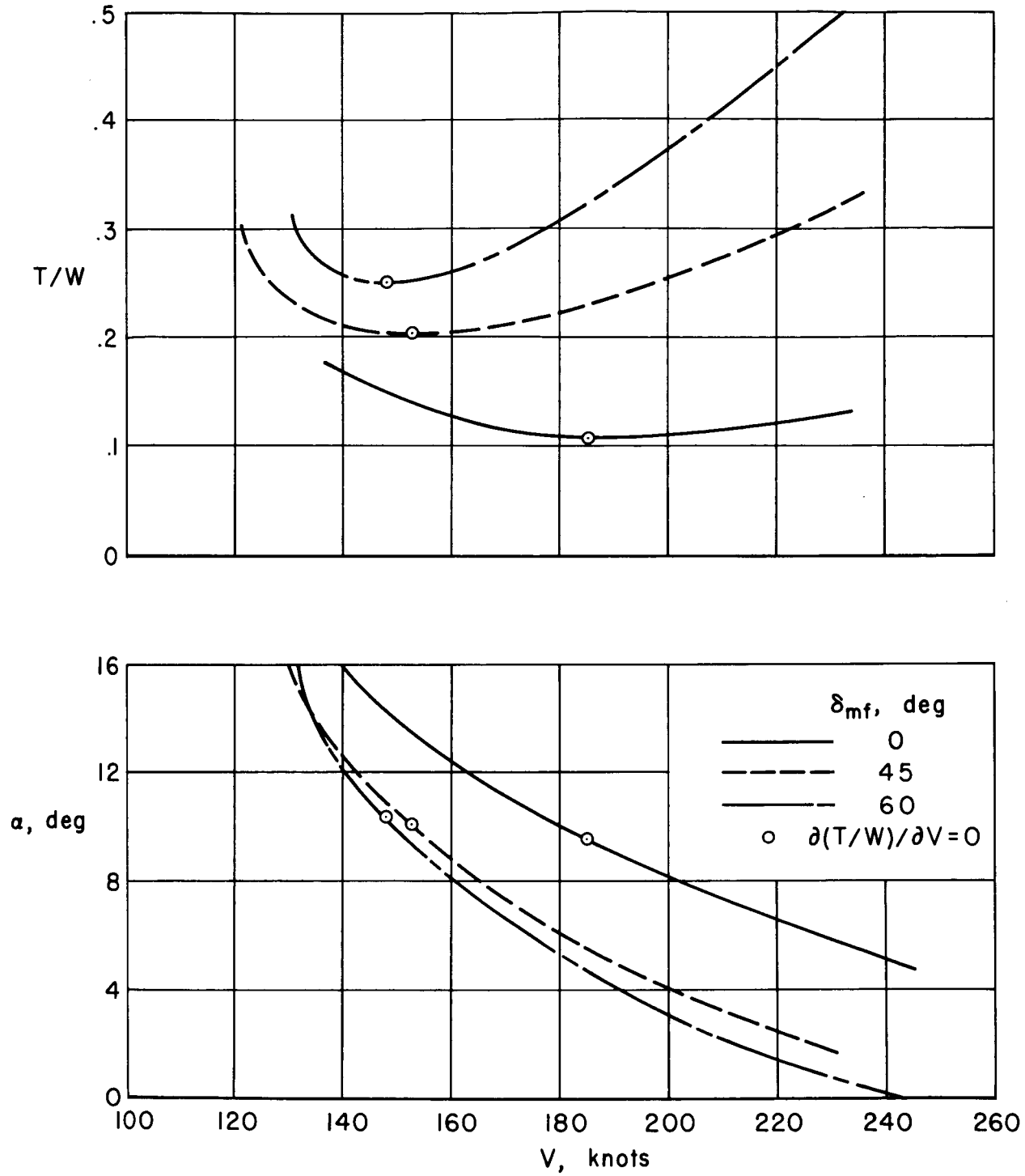

(b) $\delta_n = 45°$.

Figure 19.- Concluded.

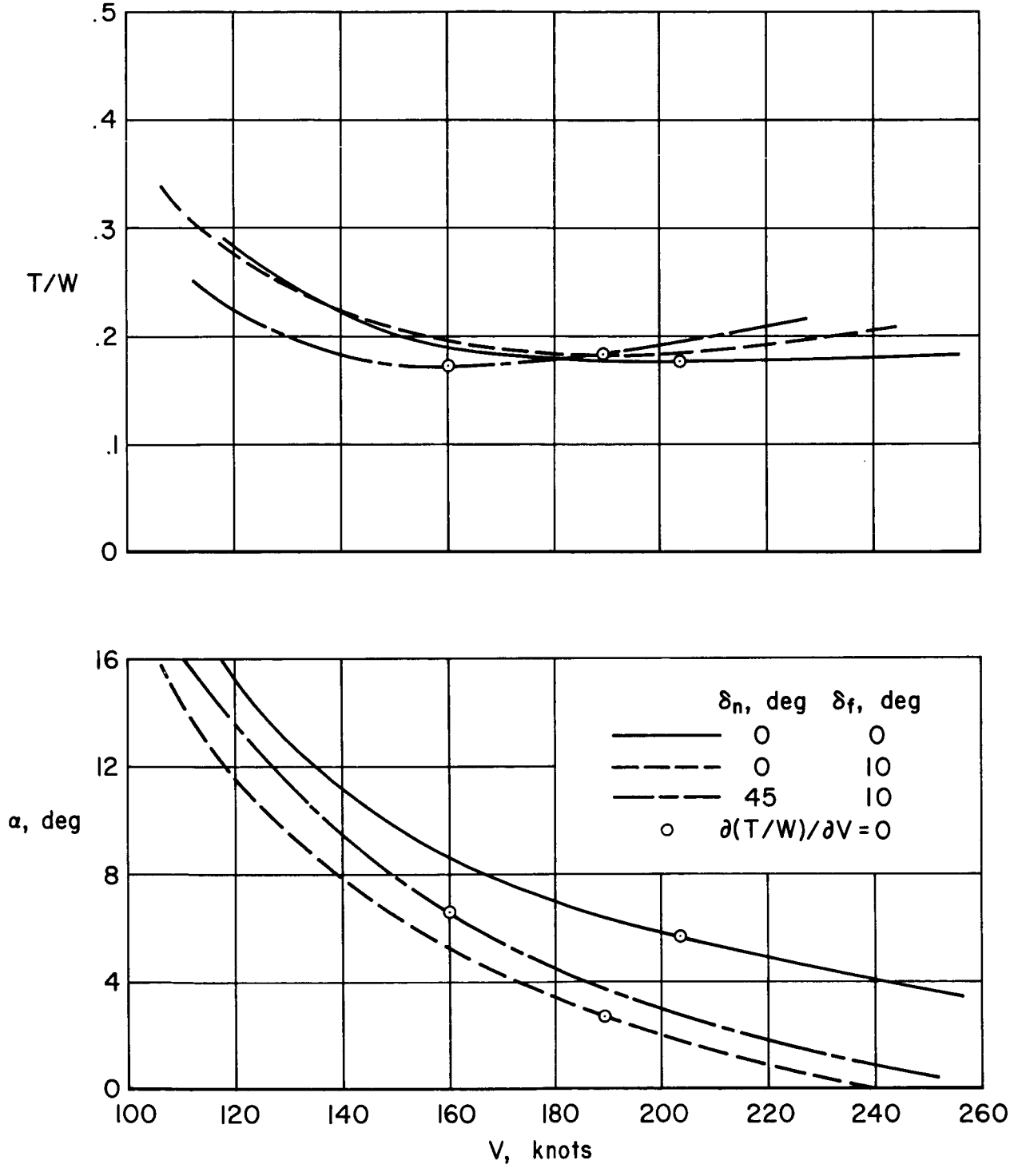

(a) $\delta_n = 0^o$; $\delta_{mf} = 0^o$.

Figure 20.- The variations of thrust-to-weight ratio and angle of attack with airspeed for the model trimmed by means of a canard control; W/S = 40 psf, MF 1(c_f/c = 0.15).

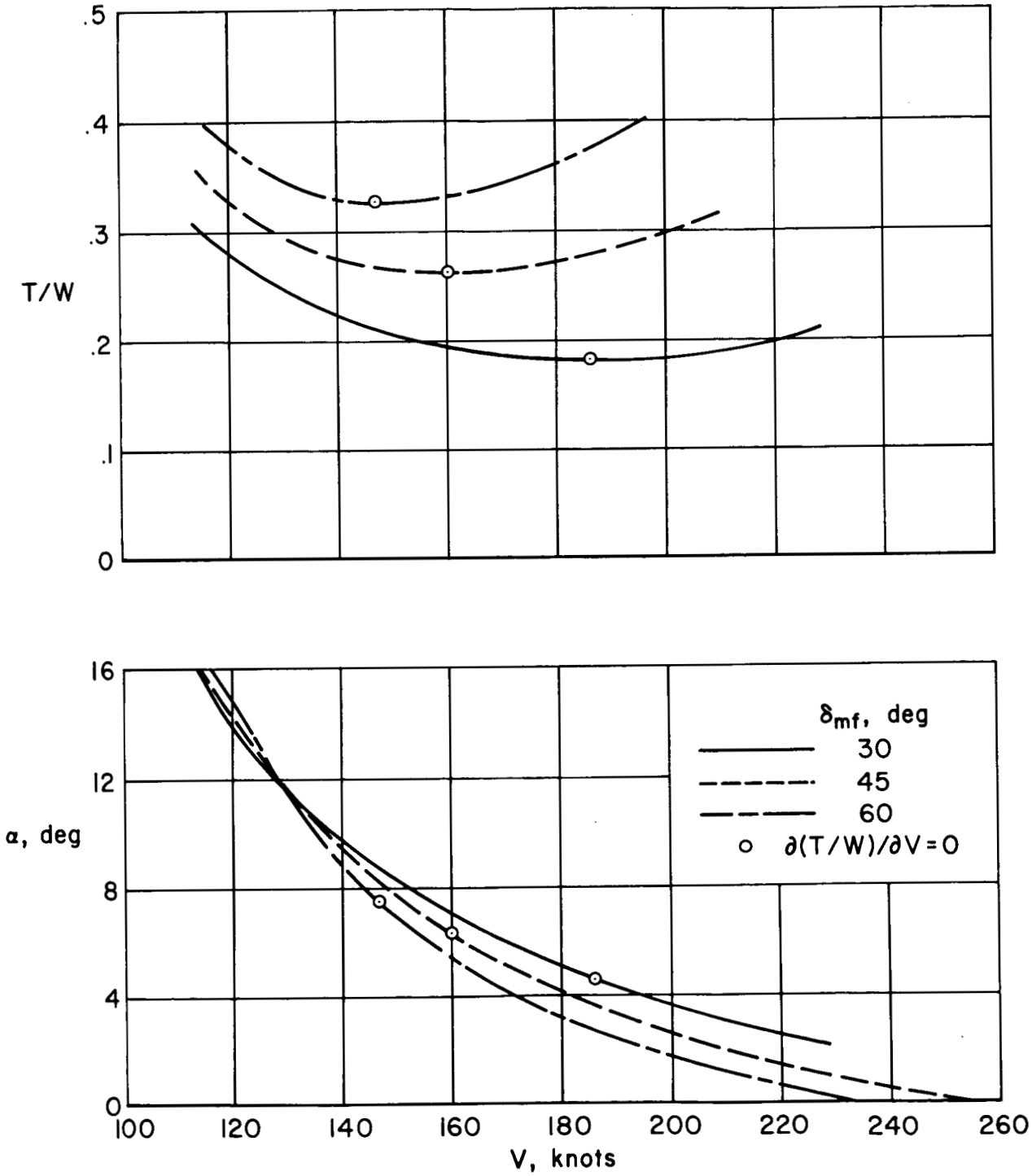

(b) $\delta_n = 0^\circ$; $\delta_f = 0^\circ$.

Figure 20.- Continued.

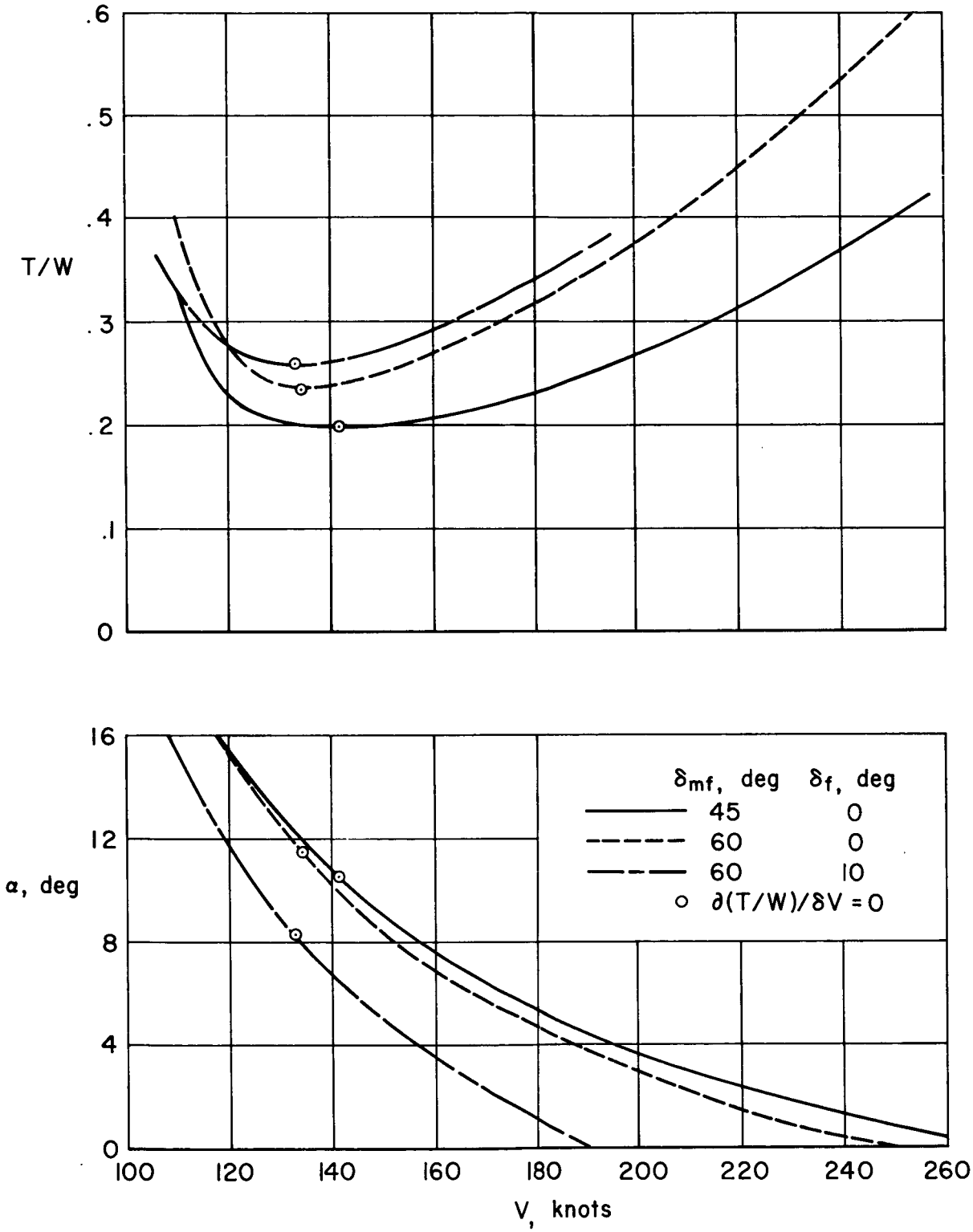

(c) $\delta_n = 45^\circ$.

Figure 20.- Concluded.

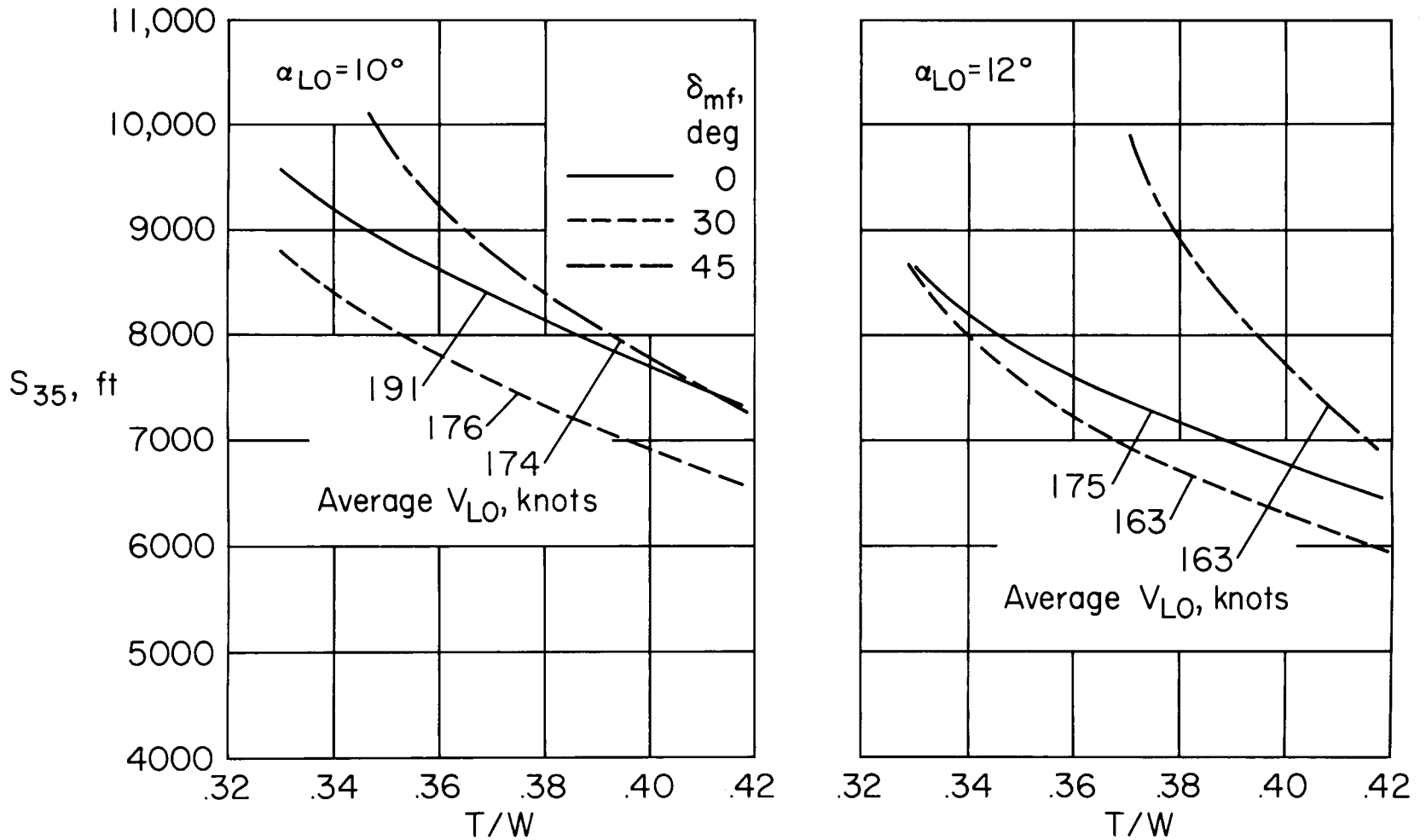

(a) Elevon controlled.

Figure 21.- The effect of flap configuration and deflection on the take-off distance required to reach an altitude of 35 feet; W/S = 70 psf, W = 450,000 lb, $\delta_n = 0°$, $c_f/c = 0.15$.

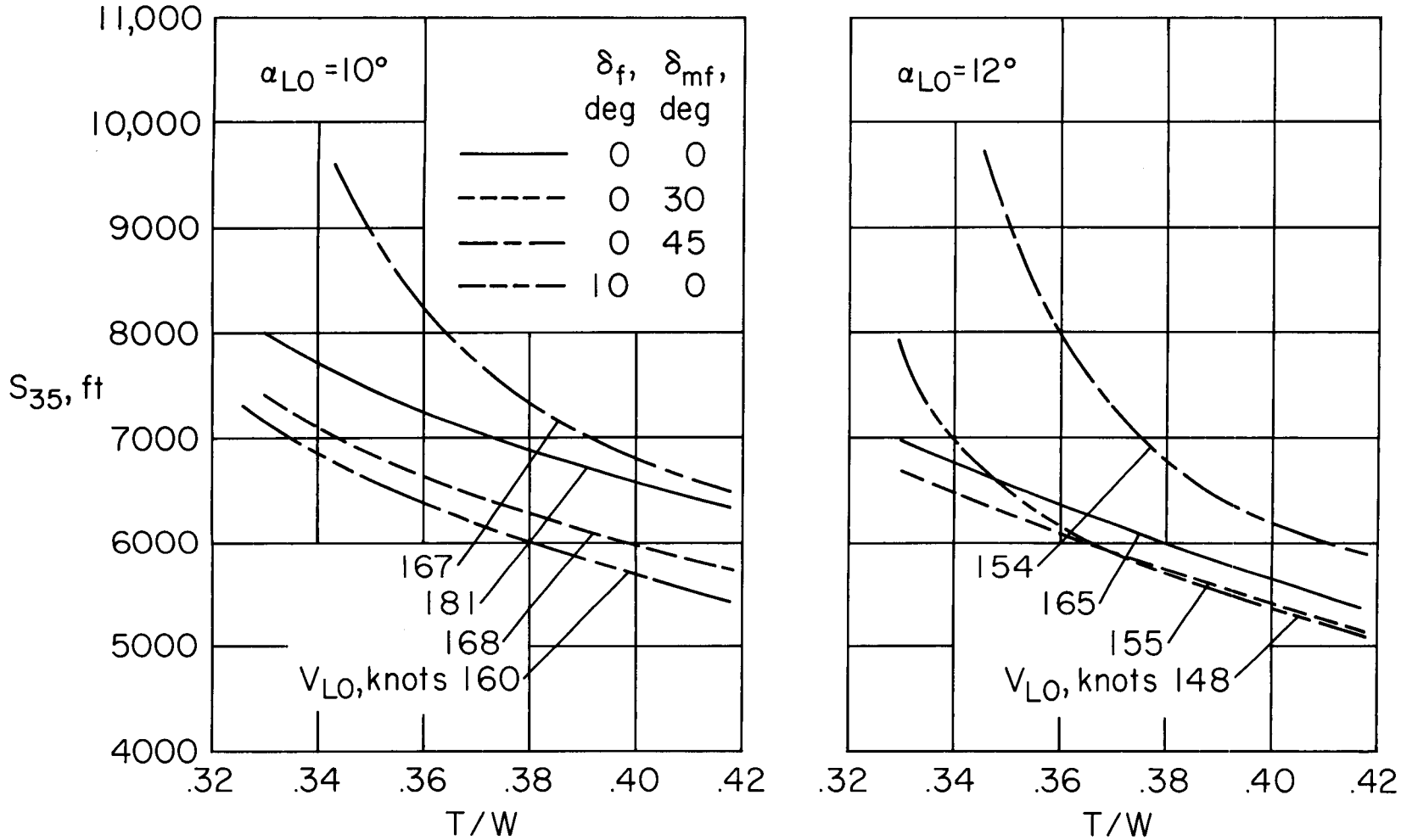

(b) Canard controlled.

Figure 21.- Concluded.

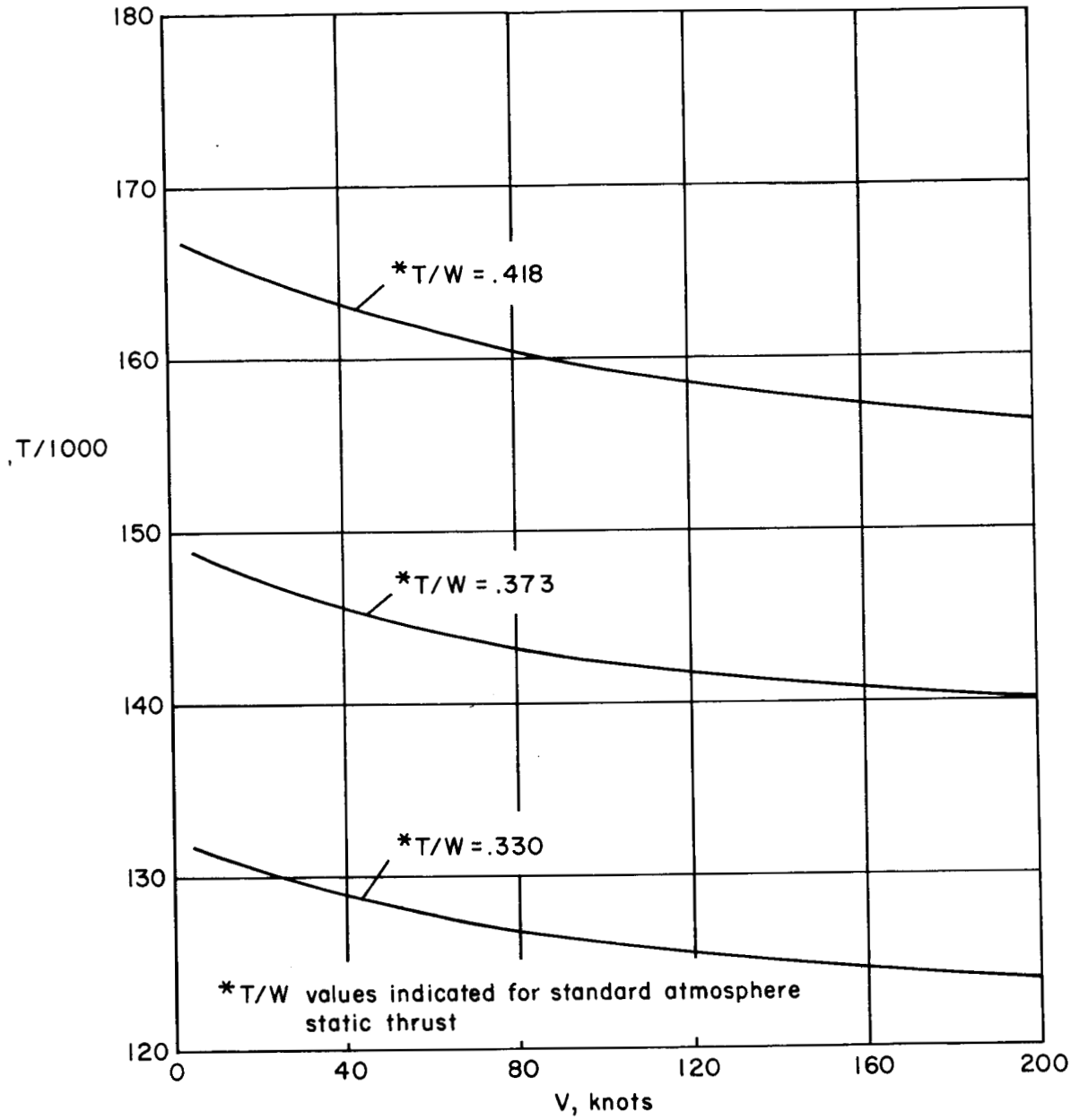

Figure 22.- The variation of hot-day thrust with airspeed used in calculation of the ground-roll and take-off distances presented in figure 21; W = 450,000 lb.